Figure 4. Growth inhibition of NSCLC cells by siRNA against *LY6K*. Response of RERF-LC-AI cells to si-*LY6K*-1 and si-*LY6K*-2 or control siRNAs (EGFP or SCR). *Left top*, the level of LY6K protein expression detected by Western blot analysis in cells treated with either control or si-*LY6K*s. *Left bottom*, colony formation assays using RERF-LC-AI cells transfected with si-*LY6K*-1 and si-*LY6K*-2, si-EGFP, or si-SCR. *Right*, the effect of siRNA against *LY6K* on cell viability, detected by 3-(4,5-dimethylthiazol-2-yl)-2,5-diphenyltetrazolium bromide assays. All assays were performed thrice and in triplicate wells.

with NSCLC and 52.5% of ESCC were diagnosed as positive whereas 6.8% to 9.5% of healthy volunteers were falsely diagnosed as positive. On the other hand, the sensitivity of the combination of conventional serum tumor marker, CEA and CYFRA 21-1 in the same set of serum samples, was 51.8% for NSCLC (53.0% for adenocarcinoma and 48.1% for SCC) and 34.4% for ESCC, whereas false-positive cases for either of the two tumor markers among normal volunteers (control group) were 6.8% (Supplementary Fig. S1*B* and *D*). Although additional validation with a larger set of serum samples covering various clinical stages will be necessary, the data presented here sufficiently show a potential clinical application of LY6K itself as a serologic/histochemical biomarker for lung and esophageal cancers. It should also be noted that we observed activation of *LY6K* in more than half of a series of other types of cancers, such as cervical carcinomas (data not shown), suggesting its diagnostic and therapeutic application to a wide range of tumors.

In summary, we have shown LY6K cancer-testis antigen as a potential biomarker for diagnosis of lung and esophageal cancers, as well as for monitoring patients with these diseases. LY6K, combined with other tumor markers, could significantly improve the sensitivity of cancer diagnosis, whereas it could be used at initial diagnosis to identify patients who might benefit from early systemic treatment. Moreover, LY6K is likely to be an essential contributor to aggressive features of NSCLC and ESCC and a likely target for development of therapeutic approaches, such as molecular targeted drugs and immunotherapy to any types of cancers overexpressing this molecule.

Acknowledgments

References

1. Berwick M. Schantz S. Chemoprevention of aerodigestive cancer. Cancer Metastasis Rev 1997;16:329–47.
2. Jemal A. Siegel R, Ward E, et al. Cancer statistics, 2006. CA Cancer J Clin 2006;56:106–30.
3. Shimada H, Nabeya Y, Ochiai T, et al. Prediction of survival with squamous cell carcinoma antigen in patients with reseable esophageal squamous cell carcinoma. Surgery 2003;133:486–94.
4. Tamoto E, Tada M, Murakawa K. et al. Gene-expression profile changes correlated with tumor progression and lymph node metastasis in esophageal cancer. Clin Cancer Res 2004;10:3629–38.
5. Parkin DM. Global cancer statistics in the year 2000. Lancet Oncol 2001;2:533–43.
6. Naruke T, Tsuchiya R, Kondo H. Asamura H. Prognosis and survival after resection for bronchogenic carcinoma based on the 1997 TNM-staging classification: the Japanese experience. Ann Thorac Surg 2001;71:1759–64.
7. Rastel D, Ramaioli A, Cornillie F, Thirion B. CYFRA 21-1, a sensitive and specific new tumour marker for squamous cell lung cancer. Report of the first European multicentre evaluation. CYFRA 21-1 Multicentre Study Group. Eur J Cancer 1994;30A:601–6.
8. Kawaguchi H. Ohno S, Miyazaki M, et al. CYFRA 21-1 determination in patients with esophageal squamous cell carcinoma: clinical utility for detection of recurrences. Cancer 2000;89:1413–7.

9. Boon T, Old LJ. Cancer tumor antigens. Curr Opin Immunol 1997;9:681–3.
10. Scanlan MJ, Simpson AJ, Old LJ. The cancer/testis genes: review, standardization, and commentary. Cancer Immun 2004;4:1.
11. Kakiuchi S, Daigo Y, Tsunoda T, Yano S, Sone S, Nakamura Y. Genome-wide analysis of organ-preferential metastasis of human small cell lung cancer in mice. Mol Cancer Res 2003;1:485–99.
12. Kikuchi T, Daigo Y, Katagiri T, et al. Expression profiles of non-small cell lung cancers on cDNA microarrays: identification of genes for prediction of lymph-node metastasis and sensitivity to anti-cancer drugs. Oncogene 2003;22:2192–205.
13. Kakiuchi S, Daigo Y, Ishikawa N, et al. Prediction of sensitivity of advanced non-small cell lung cancers to gefitinib (Iressa, ZD1839). Hum Mol Genet 2004;13: 3029–43.
14. Kikuchi T, Daigo Y, Ishikawa N, et al. Expression profiles of metastatic brain tumor from lung adenocarcinomas on cDNA microarray. Int J Oncol 2006;28: 799–805.
15. Taniwaki M, Daigo Y, Ishikawa N, et al. Gene expression profiles of small-cell lung cancers: molecular signatures of lung cancer. Int J Oncol 2006;29: 567–75.
16. Yamabuki T, Daigo Y, Kato T, et al. Genome-wide gene expression profile analysis of esophageal squamous-cell carcinomas. Int J Oncol 2006;28:1375–84.

17. Saito-Hisaminato A, Katagiri T, Kakiuchi S, Nakamura T, Tsunoda T, Nakamura Y. Genome-wide profiling of gene expression in 29 normal human tissues with a cDNA microarray. DNA Res 2002;9:35–45.
18. Ochi K, Daigo Y, Katagiri T, et al. Expression profiles of two types of human knee joint cartilage. J Hum Genet 2003;48:177–82.
19. Suzuki C, Daigo Y, Kikuchi T, Katagiri T, Nakamura Y. Identification of COX17 as a therapeutic target for non-small cell lung cancer. Cancer Res 2003;63:7038–41.
20. Ishikawa N, Daigo Y, Yasui W, et al. ADAM8 as a novel serological and histochemical marker for lung cancer. Clin Cancer Res 2004;10:8363–70.
21. Kato T, Daigo Y, Hayama S, et al. A novel human tRNA-dihydrouridine synthase involved in pulmonary carcinogenesis. Cancer Res 2005;65:5638–46.
22. Furukawa C, Daigo Y, Ishikawa N, et al. Plakophilin 3 oncogene as prognostic marker and therapeutic target for lung cancer. Cancer Res 2005;65:7102–10.
23. Ishikawa N, Daigo Y, Takano A, et al. Increases of amphiregulin and transforming growth factor-α in serum as predictors of poor response to gefitinib among patients with advanced non-small cell lung cancers. Cancer Res 2005;65:9176–84.
24. Suzuki C, Daigo Y, Ishikawa N, et al. ANLN plays a critical role in human lung carcinogenesis through the activation of RHOA and by involvement in the phosphoinositide 3-kinase/AKT pathway. Cancer Res 2005;65:11314–25.

25. Ishikawa N, Daigo Y, Takano A, et al. Characterization of SEZ6L2 cell-surface protein as a novel prognostic marker for lung cancer. Cancer Sci 2006;97:737–45.

26. Takahashi K, Furukawa C, Takano A, et al. The neuromedin u-growth hormone secretagogue receptor 1b/neurotensin receptor 1 oncogenic signaling pathway as a therapeutic target for lung cancer. Cancer Res 2006; 66:9408–19.

27. Hayama S, Daigo Y, Kato T, et al. Activation of CDCA1-2, members of centromere protein complex, involved in pulmonary carcinogenesis. Cancer Res 2006; 66:10339–48.

28. Kato T, Hayama S, Yamabuki Y, et al. Increased expression of insulin-like growth factor-II messenger RNA-binding protein 1 is associated with tumor progression in patients with lung cancer. Clin Cancer Res 2007;13:434–42.

29. Suzuki C, Takahashi K, Hayama S, et al. Identification of Myc-associated protein with JmjC domain as a novel therapeutic target oncogene for lung cancer. Mol Cancer Ther 2007;6:542–51.

30. Yamabuki T, Takano A, Hayama S, et al. Dickkopf-1 as a novel serologic and prognostic biomarker for lung and esophageal carcinomas. Cancer Res 2007;67: 2517–25.

31. Hayama S, Daigo Y, Yamabuki T, et al. Phosphorylation and activation of cell division cycle associated 8 by aurora kinase B plays a significant role in human lung carcinogenesis. Cancer Res 2007;67:4113–22.

32. Kato T, Sato N, Hayama S, et al. Activation of holiday junction-recognizing protein involved in the chromosomal stability and immortality of cancer cells. Cancer Res 2007;67:8544–53.

33. Taniwaki M, Takano A, Ishikawa N, et al. Activation of KIF4A as a Prognostic Biomarker and Therapeutic Target for Lung Cancer. Clin Cancer Res. In press 2007.

34. de Nooij-van Dalen AG, van Dongen GA, Smeets SJ, et al. Characterization of the human Ly-6 antigens, the newly annotated member Ly-6K included, as molecular markers for head-and-neck squamous cell carcinoma. Int J Cancer 2003;103:768–74.

35. Lee JW, Lee YS, Yoo KH, et al. LY-6K gene: a novel molecular marker for human breast cancer. Oncol Rep 2006;16:1211–4.

36. Travis WD, Colby TV, Corrin B, Shimosato Y, Brambilla E. Histological Typing of Lung and Pleural Tumors: World Health Organization International Histological Classification of Tumors. 3rd ed. Berlin: Springer; 1999.

37. Chin SF, Daigo Y, Huang HE, et al. A simple and reliable pretreatment protocol facilitates fluorescent *in situ* hybridisation on tissue microarrays of paraffin wax embedded tumour samples. Mol Pathol 2003;56: 275–9.

38. Callagy G, Cattaneo E, Daigo Y, et al. Molecular classification of breast carcinomas using tissue microarrays. Diagn Mol Pathol 2003;12:27–34.

39. Callagy G, Pharoah P, Chin SF, et al. Identification and validation of prognostic markers in breast cancer with the complementary use of array-CGH and tissue microarrays. J Pathol 2005;205:388–96.

40. Nakatsura T, Yoshitake Y, Senju S, et al. Glypican-3, overexpressed specifically in human hepatocellular carcinoma, is a novel tumor marker. Biochem Biophys Res Commun 2003;306:16–25.

41. Bamezai A, Rock KL. Overexpressed Ly-6A.2 mediates cell-cell adhesion by binding a ligand expressed on lymphoid cells. Proc Natl Acad Sci U S A 1995;92:4294–8.

42. Balsara BR, Sonoda G, du Manoir S, Siegfried JM, Gabrielson E, Testa JR. Comparative genomic hybridization analysis detects frequent, often high-level, overrepresentation of DNA sequences at 3q, 5p, 7p,

and 8q in human non-small cell lung carcinomas. Cancer Res 1997;57:2116–20.

43. Gold P, Freedman S. Demonstration of tumor-specific antigens in human colonic carcinomata by immunological tolerance and absorption techniques. J Exp Med 1965;121:439–62.

44. Hammarstrom S. The carcinoembryonic antigen (CEA) family: structures, suggested functions and expression in normal and malignant tissues. Semin Cancer Biol 1999;9:67–81.

45. Hashimoto M, Ichihara M, Watanabe T, et al. Expression of CD109 in human cancer. Oncogene 2004;23:3716–20.

46. Jantscheff P, Terracciano L, Lowy A, et al. Expression of CEACAM6 in resectable colorectal cancer: a factor of independent prognostic significance. J Clin Oncol 2003; 21:3638–46.

47. Reiter RE, Gu Z, Watabe T, et al. Prostate stem cell antigen: a cell surface marker overexpressed in prostate cancer. Proc Natl Acad Sci U S A 1998;95:1735–40.

48. Marshall JL, Gulley JL, Arlen PM, et al. Phase I study of sequential vaccinations with fowlpox-CEA(6D)-TRI-COM alone and sequentially with vaccinia-CEA(6D)-TRICOM, with and without granulocyte-macrophage colony-stimulating factor, in patients with carcinoembryonic antigen-expressing carcinomas. J Clin Oncol 2005;23:720–31.

49. Ross S, Spencer SD, Holcomb I, et al. Prostate stem cell antigen as therapy target: tissue expression and *in vivo* efficacy of an immunoconjugate. Cancer Res 2002;62:2546–53.

50. Saffran DC, Raitano AB, Hubert RS, Witte ON, Reiter RE, Jakobovits A. Anti-PSCA mAbs inhibit tumor growth and metastasis formation and prolong the survival of mice bearing human prostate cancer xenografts. Proc Natl Acad Sci U S A 2001;98:2658–63.

Melanoma-associated antigen-A1 expression predicts resistance to docetaxel and paclitaxel in advanced and recurrent gastric cancer

TAKAHISA SUZUKI[1], KAZUHIRO YOSHIDA[1], YOSHIYUKI WADA[1], YOICHI HAMAI[1], KAZUHIRO SENTANI[2], NAOHIDE OUE[2] and WATARU YASUI[2]

[1]Department of Surgical Oncology, Research Institute for Radiation Biology and Medicine, Hiroshima University;
[2]Department of Molecular Pathology, Hiroshima University Graduate School of Biomedical Sciences, Hiroshima, Japan

Abstract. Melanoma-associated antigen (*MAGE*) genes are cancer-testis antigen genes that serve as immunotherapy targets in several human cancers. Previous studies have revealed that the forced expression of *MAGE* genes induces a paclitaxel-resistant phenotype. In the present study, we examined whether the expression of MAGE-A1 could predict the response of advanced and recurrent gastric cancers (GCs) to taxan (docetaxel or paclitaxel)-based chemotherapy. The expression of MAGE-A1 was analyzed by immunostaining in 41 primary GC samples. DNA demethylation was assessed by methylation-specific polymerase chain reaction and the effect of the forced expression of MAGE-A1 on drug resistance to taxan drugs was monitored by MTT assay. The expression of MAGE-A1 in primary GC was observed in 4 (9.8%) of 41 cases. All 4 patients with MAGE-A1-positive GC showed progressive disease, whereas MAGE-A1 expression was not detected in any of the 23 patients showing partial response (P=0.0302). There was no association between *MAGE-A1* gene demethylation and response to chemotherapy (P=0.7245). The forced MAGE-A1 expression in the TMK-1 GC cell line increased the sensitivity to paclitaxel and docetaxel. These results suggest that although MAGE-A1 does not participate directly in the drug-resistant phenotype, the expression of MAGE-A1 could be a marker for the prediction of resistance to taxan-based chemotherapies in patients with GC.

Introduction

Gastric cancer (GC) is one of the most common cancers worldwide. Despite improvements in cancer diagnosis and therapy, many patients are still diagnosed at the late stages of

Correspondence to: Dr Wataru Yasui, Department of Molecular Pathology, Hiroshima University Graduate School of Biomedical Sciences, 1-2-3 Kasumi, Minami-ku, Hiroshima 734-8551, Japan
E-mail: wyasui@hiroshima-u.ac.jp

the disease, and the disease often recurs even after curative surgery. Until recently, GC was considered a poorly chemo-responsive cancer. However, several clinical trials have shown that certain chemotherapeutic agents are quite effective against GC. We recently reported that a combination of docetaxel and S-1 is active against metastatic GC (1,2). The taxoids, paclitaxel (taxol) and docetaxel (taxotere), are promising antitumor compounds. Paclitaxel and docetaxel work as mitotic spindle toxins, that stabilize microtubules and enhance microtubule polymerization, resulting in the mitotic arrest of tumor cells (3). S-1 is an oral fluorouracil antitumor drug that contains a combination of three pharmacological agents. Although combination chemotherapy with docetaxel and S-1 has shown a high degree of efficacy against GC (4), some patients have shown a poor response, possibly due to the inefficiency of the chemotherapy. For effective treatment, the identification of patients who will respond well to a specific chemotherapy could be important. Therefore, there is an urgent need for new biomarkers for GC chemotherapy.

Cancer develops as a result of multiple genetic and epigenetic alterations (5,6). Better knowledge of the changes in gene expression that occur during gastric carcinogenesis could lead to improvements in diagnosis, treatment and prevention. In order to identify potential molecular markers for GC and to better understand the development of GC at the molecular level, comprehensive analyses of gene expression could be useful (7). We previously performed serial analysis of gene expression (SAGE) of 4 primary GCs (8) and identified several GC-specific genes (9). Of these genes, *taxol* (also known as paclitaxel) *resistance associated gene 3* [*TRAG3*, also known as *CSAG family, member 2* (*CSAG2*)] is a candidate gene for cancer-specific expression, at least in patients with GC. *TRAG3* was originally identified by the differential gene expression of SKOV-3 and its taxol-resistant subline, SKOV-3_{TR}. However, the expression of endogenous TRAG3 in taxol-sensitive cell lines does not confer taxol resistance, suggesting that TRAG3 does not participate directly in the taxol-resistant phenotype (10). TRAG3 is a cancer-testis antigen and is overexpressed in malignant melanoma (11), colorectal (12), lung (13), and breast cancer (14). Although TRAG3 has been identified as a T-lymphocyte epitope (15), the biological function of TRAG3 is poorly understood. *TRAG3* is located on chromosome Xq28 and is flanked by the *melanoma-associated antigen* (*MAGE*) gene

cluster, which includes *MAGE-2, 3, 4, 5, 10*, and *12*. It has been reported that both MAGE-2 (also known as MAGE-A2) and MAGE-6 (also known as MAGE-A6) transfectants demonstrate a 4-fold increase in resistance to paclitaxel (16). Therefore, the acquisition of paclitaxel resistance could be associated with the increased expression of *MAGE* but not *TRAG3*. *MAGE* genes are considered tumor-specific antigens and ideal targets for cancer immunotherapy (17) as they are expressed in a large variety of neoplastic lesions and only in the testes in healthy adults (18). However, the clinical utility of the expression of *MAGE* genes for the prediction of chemosensitivity has not been investigated in cancers including GC.

In the present retrospective study, the relationship between the expression of *MAGE-A1* (also known as MAGE-1) and the response of advanced and recurrent GCs to chemotherapy with paclitaxel or docetaxel was investigated. As the expression of *MAGE-A1* is activated by DNA demethylation in GC (19), the DNA methylation status of *MAGE-A1* was also analyzed by methylation-specific polymerase chain reaction (PCR).

Patients and methods

Patients and tumor specimens. The subjects were 41 patients with GC referred to the Department of Surgical Oncology, Hiroshima University Hospital (Hiroshima, Japan). Forty-one GC tissue samples and 41 corresponding non-neoplastic mucosa samples from these 41 patients were analyzed for the expression and DNA methylation of *MAGE-A1*. The GC and the corresponding non-neoplastic mucosa samples were obtained by resection or biopsy before the initiation of chemotherapy. All 41 specimens were archival, formalin-fixed, paraffin-embedded tissues. We confirmed microscopically that the tumor tissue specimens consisted mainly (>50%) of cancer cells and that the non-neoplastic mucosae did not show any evidence of tumor cell invasion or significant inflammatory involvement. All patients were determined to have inoperable or recurrent GC. Of the 41 patients, 12 were treated with paclitaxel alone; the remaining 29 were treated with a combination of docetaxel and S-1.

Paclitaxel (80 mg/m2) was infused over 1 h on days 1, 8, and 15, followed by a 1-week interval (1 cycle). For the combination therapy of S-1 and docetaxel (2), S-1 was administered orally at a dose of 80 mg/m^2 within 30 min of the morning and evening meals for 2 weeks, followed by a 1-week interval (1 cycle). Docetaxel (40 mg/m^2) in 100 ml 0.9% saline was infused over 1 h on the morning of day 1. This cycle of administration was repeated every 3 weeks, and the infusion was started at the same time as the S-1 administration.

All 41 patients provided a medical history and underwent a physical examination including an evaluation of performance status, complete blood cell count (CBC), serum chemistry profile, creatinine clearance, urinalysis, electrocardiography, chest X-ray, and computed tomography (CT) and/or magnetic resonance imaging at the time of enrollment. An upper GI series, gastrointestinal fiberscopy (GIF), and barium enema were performed if necessary. A baseline biological analysis (CBC, serum chemistry profile and urinalysis) and a physical examination, including the determination of weight and performance status, was performed at least weekly while the

patients were undergoing treatment. Tumor markers, including CEA and CA19-9, were checked once each month.

The responses of the primary and metastatic lesions to treatment were assessed according to the World Health Organization criteria. The primary and metastatic lesions were evaluated by GIF, CT, ultrasonography, and other radiographic examinations. Complete response (CR) was defined as the absence of all evidence of cancer for <4 weeks. Partial response (PR) was defined as at least 50% reduction in the sum of the products of the perpendicular diameters of all lesions for <4 weeks without any evidence of new lesions or the progression of existing lesions. No change (NC) was defined as <50% reduction or <25% increase in the sum of the products of the perpendicular diameters of all lesions without any evidence of new lesions. Progressive disease (PD) was defined as >25% increase in <1 lesion or the appearance of new lesions. Of the 12 patients treated with paclitaxel alone, none showed CR, 4 showed PR, 5 showed NC, and 3 showed PD. Of the 29 patients treated with the combination of docetaxel and S-1, none showed CR, 19 showed PR, 4 showed NC, and 6 showed PD.

Histological classification (intestinal-type or diffuse-type) was performed according to the Lauren classification system (20). Tumor staging was according to the TNM staging system (21). As written informed consent had not been obtained for the use of some samples, the identifying information was removed from all the samples prior to analysis to protect patient privacy. This procedure was in accordance with the Ethical Guidelines for Human Genome/Gene Research enacted by the Japanese Government.

Immunohistochemistry. Formalin-fixed, paraffin-embedded samples (primary GC) were sectioned, deparaffinized, stained with H&E, and evaluated to ensure that the sectioned block contained tumor cells. Adjacent sections were then stained immunohistochemically. For immunostaining of MAGE-A1, a Dako LSAB Kit (Dako, Carpinteria, CA, USA) was used according to the manufacturer's recommendations. In brief, the sections were pretreated by microwaving them in citrate buffer for 30 min to retrieve antigenicity. After peroxidase activity was blocked with 3% H_2O_2-methanol for 10 min, the sections were incubated with normal goat serum (Dako) for 20 min to block nonspecific antibody binding sites. Anti-MAGE-1 antibody (6C1, 1:100, Novocastra, Newcastle, UK) was incubated with tissue samples for 60 min at room temperature, followed by incubations with biotinylated anti-rabbit/mouse IgG and peroxidase-labeled streptavidin for 10 min each. Staining was completed with a 10-min incubation with the substrate-chromogen solution. The sections were counterstained with 0.1% hematoxylin. The 6C1 antibody recognizes both the MAGE-A1 protein and the MAGE-A10 protein (22). It has been confirmed that MAGE-A10 is present in the nucleus, whereas MAGE-A1 is localized in the cytoplasm (22). Therefore, cytoplasmic staining was considered positive for MAGE-A1, and nuclear staining was disregarded in the present study.

Genomic DNA extraction and methylation-specific PCR (MSP). For DNA extraction from the archival, formalin-fixed, paraffin-embedded tissue samples, primary GC samples and
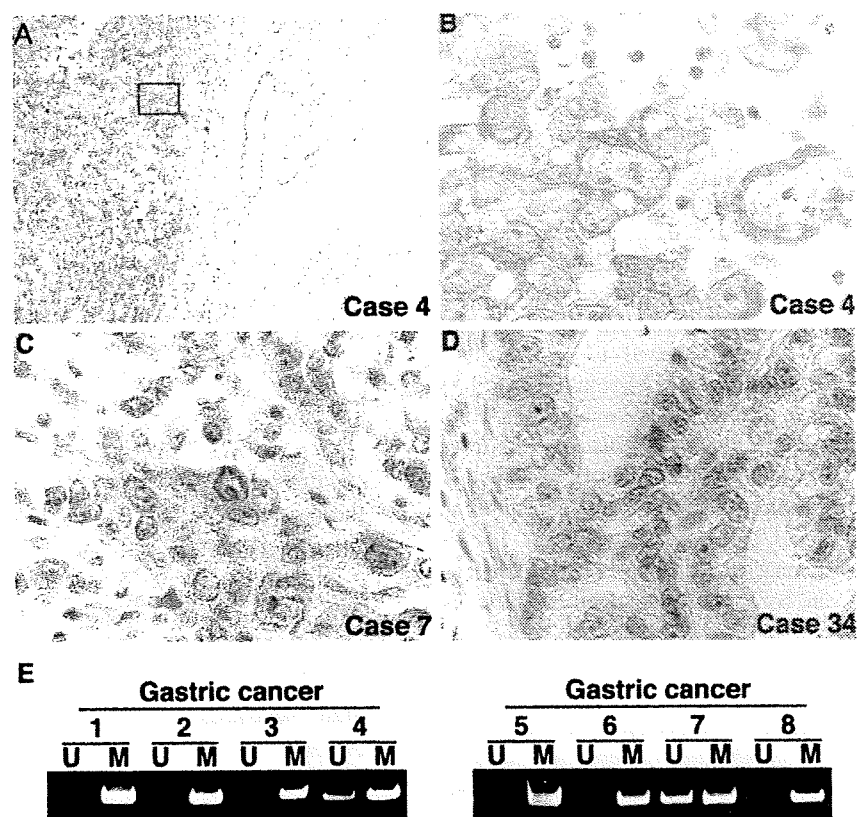
Figure 1. Melanoma-associated antigen-A1 (MAGE-A1) expression in gastric cancer (GC). (A) Sections of GC and the corresponding non-neoplastic mucosae were immunostained with monoclonal antibody 6C1. In the corresponding non-neoplastic gastric mucosae, no staining was detected, whereas strong and extensive staining was observed in the GC cells (original magnification, x100). Panel (B) is a high-magnification view of the field indicated by the box in panel (A) (original magnification, x1000). Only cytoplasmic staining is visible in Case 4, and therefore, this case was considered positive for MAGE-A1 expression. Stromal cells were not stained. (C) In Case 7, both the nuclear and cytoplasmic staining of MAGE-A1 were observed. GC cases showing both cytoplasmic and nuclear staining were considered positive for MAGE-A1 immunostaining (original magnification, x1000). (D) In Case 34, only nuclear staining is visible. GC cases showing only nuclear staining were considered negative for MAGE-A1 expression (original magnification, x1000). (E) DNA methylation analyses of MAGE-A1 in the GC tissues by methylation-specific polymerase chain reaction (MSP). Primer sets were used, unmethylated (U), methylated (M). The methylated allele was present in all the cases. The unmethylated allele was detected in Cases 4 and 7. The expression of MAGE-A1 was observed in Cases 4 (B) and 7 (C) by immunostaining.

corresponding non-neoplastic samples were manually dissected with a fine needle from different sets of 10 serial, 10-μm-thick, formalin-fixed, paraffin-embedded tissue sections. The dissected samples were lysed by incubation in 200 mg/ml proteinase K at 55°C for 3 days. Genomic DNA was purified by 3 rounds of phenol/chloroform extraction followed by ethanol precipitation. In order to examine DNA methylation patterns, genomic DNA was treated with 3 M sodium bisulfite as described previously (23). For analysis of DNA methylation of the MAGE-A1 gene, MSP was performed as described previously (19). The PCR products (15 μl) were separated on 8% non-denaturing polyacrylamide gels, stained with ethidium bromide, and visualized under ultraviolet light.

Cell lines, expression vector, and transfection. The TMK-1 GC cell line was established in our laboratory (24). All cell lines were maintained in RPMI-1640 (Nissui Pharmaceutical, Tokyo, Japan) containing 10% fetal bovine serum (Whittaker, Walkersville, MD, USA) in a humidified atmosphere of 5% CO_2 and 95% air at 37°C. For constitutive expression of the MAGE-A1 gene, cDNA was PCR amplified and subcloned

into pcDNA 3.1 (Invitrogen, Carlsbad, CA, USA). The pcDNA-MAGE-A1 expression vector was transfected into TMK-1 cells with FuGENE6 (Roche Diagnostics, Indianapolis, IN, USA) according to the manufacturer's instructions. Stable transfectants were selected after 2 weeks of culture with 80 μg/ml G418 (Invitrogen).

Western blot analysis. The preparation of whole-cell lysates and Western blot analysis were performed as described previously (25). Protein concentrations were determined by the Bradford protein assay (Bio-Rad, Richmond, CA, USA) with bovine serum albumin used as the standard. Lysates (40 μg) were solubilized in Laemmli's sample buffer by boiling and then subjected to 10% SDS-polyacrylamide gel electrophoresis followed by electrotransfer onto a nitrocellulose filter. The filter was incubated for 1 h at room temperature with an anti-MAGE-A1 antibody. Peroxidase-conjugated anti-mouse IgG was used in the secondary reaction. The immunocomplexes were visualized with an ECL Western Blot Detection System (Amersham Biosciences, Piscataway, NJ, USA). The quality and amounts of proteins

on the gel were confirmed by detection with an anti-ß-actin antibody (Sigma Chemical Co., St. Louis, MO, USA).

Drug treatment and cell growth assay. Docetaxel was obtained from Rhone-Poulenc Rorer (Antony, France). Paclitaxel and mitomycin C were purchased from Sigma. Cell growth was assessed by a standard 3-(4,5-dimethyl-2-tetrazolyl)-2,5-diphenyl-2H tetrazoluim bromide (MTT) assay as described previously (4). In brief, GC cells were seeded into 96-well culture plates. After 24-h incubation, the cells were incubated for 72 h at 37°C with varied drug concentrations (0.1-100 nM docetaxel, 0.1-100 nM paclitaxel, and 0.01-10 μM mitomycin C). After incubation, 10 μl MTT (Sigma) solution (5 mg/ml) were added to each well, and the plates were incubated for 3 h at 37°C. The growth medium was then replaced with 150 μl dimethyl sulfoxide (Wako, Tokyo, Japan) per well, and the absorbance at 540 nm was measured with a Titertek Multiscan.

Statistical methods. Differences were analyzed by Fisher's exact test. P-values <0.05 were considered statistically significant.

Results

Relationship between MAGE-A1 expression and response of GC to paclitaxel and the combination of docetaxel and S-1. The expression and distribution of MAGE-A1 was investigated by immunostaining of 41 GC tissues. MAGE-A1 was not stained in the corresponding non-neoplastic mucosae (Fig. 1A). Three GCs showed only cytoplasmic staining of MAGE-A1 (Fig. 1B) and both cytoplasmic and nuclear staining were observed in one GC (Fig. 1C). One GC showed only nuclear staining (Fig. 1D). As described in 'Materials and methods', cytoplasmic staining was considered positive for MAGE-A1 expression and nuclear staining was disregarded. In total, MAGE-A1 staining was observed in 4 (9.8%) of the 41 GC tissues. In all the 4 cases, >50% of the cancer cells were stained, and in the remaining 37 cases, no expression of MAGE-A1 was observed. We considered that all the 4 cases were positive for MAGE-A1. The expression of MAGE-A1 was not associated with age or sex (data not shown). There was no clear association between MAGE-A1 expression and the clinicopathological characteristics in the group of 20 GC cases obtained by resection (Table I). Of the 12 patients treated with paclitaxel alone, the 2 MAGE-A1-positive patients showed PD in response to paclitaxel, whereas 4 of the 10 MAGE-A1-negative patients showed PR. Of the 29 patients treated with a combination of docetaxel and S-1, the 2 MAGE-A1-positive patients showed PD, whereas 19 of the 27 MAGE-A1-negative patients showed PR. In total, the 4 patients with MAGE-A1-positive GC showed PD in response to taxan-based chemotherapy, and the expression of MAGE-A1 was not detected in the 23 patients showing PR to the taxan-based chemotherapy (P=0.0302, Table II). These findings indicate that the expression of MAGE-A1 is a marker for the response to taxan-based chemotherapy.

Relationship between DNA methylation of the MAGE-A1 gene and response of GC to paclitaxel and combination therapy of docetaxel and S-1. We investigated the DNA methylation status of the *MAGE-A1* gene as the expression of

Table I. Relationship between MAGE-A1 protein expression and clinicopathological characteristics in GC.

	MAGE-A1 expression		
	Positive (%)	Negative	P-value[a]
T grade			
T1/2/3	1 (7.1)	13	0.2018
T4	2 (33.3)	4	
N grade			
N0/1/2	1 (9.1)	10	0.5658
N3	2 (22.2)	7	
Liver metastasis			
Present	0 (0)	5	0.5395
Absent	3 (20)	12	
Peritoneal dissemination			
Present	1 (16.7)	5	1.0000
Absent	2 (14.3)	12	
Distant metastasis			
Present	0 (0)	0	ND
Absent	3 (15)	17	
Stage			
I/II/III	1 (14.3)	6	1.0000
IV	2 (15.4)	11	
Histology			
Intestinal	1 (25)	3	1.0000
Diffuse	5 (31.3)	11	

MAGE-A1, melanoma-associated antigen-A1; GC, gastric cancer; ND, not determined. [a]Fisher's exact test.

Table II. Association between MAGE-A1 expression and response to taxan-based chemotherapy.

Response	No. of cases	No. of MAGE-A1-positive cases (%)	P-value[a]
CR	0	0 (0)	0.0302
PR	23	0 (0)	
NC	9	0 (0)	
PD	9	4 (44.4)	

MAGE-A1, melanoma-associated antigen-A1; CR, complete response; PR, partial response; NC, no change; PD, progressive disease. [a]Fisher's exact test (CR plus PR vs NC plus PD).

MAGE-A1 is activated by DNA demethylation in GC (19). Representative results of MSP are shown in Fig. 1E. In total, the DNA demethylation of *MAGE-A1* was detected in 10

Table III. Relationship between DNA demethylation of MAGE-A1 and clinicopathological characteristics in GC.

| | MAGE-A1 methylation status | | |
	Demethyl- ated (%)	Methyl- ated	P-value[a]
T grade			
T1/2/3	3 (21.4)	11	0.3027
T4	3 (50)	3	
N grade			
N0/1/2	4 (36.4)	7	0.6424
N3	2 (22.2)	7	
Liver metastasis			
Present	1 (20)	4	1.0000
Absent	5 (33.3)	10	
Peritoneal dissemination			
Present	2 (33.3)	4	1.0000
Absent	4 (28.6)	10	
Distant metastasis			
Present	0 (0)	0	ND
Absent	6 (30)	14	
Stage			
I/II/III	2 (28.6)	5	1.0000
IV	4 (30.8)	9	
Histology			
Intestinal	0 (0)	4	1.0000
Diffuse	3 (18.8)	13	

MAGE-A1, melanoma-associated antigen-A1; GC, gastric cancer; ND, not determined. [a]Fisher's exact test.

Table IV. Relationship between DNA demethylation of MAGE-A1 and expression of MAGE-A1.

| | MAGE-A1 methylation status | | |
MAGE-A1 expression	Demethyl- ated (%)	Methyl- ated	P-value[a]
Positive	4 (100)	0	0.034
Negative	6 (16.2)	31	

MAGE-A1, melanoma-associated antigen-A1. [a]Fisher's exact test.

(24.4%) of the 41 GC samples. The demethylation of MAGE-A1 was not associated with patient age or sex (data not shown). There was no clear association between the demethylation of MAGE-A1 and clinicopathological characteristics in the group of 20 GC cases obtained by resection (Table III).

Table V. Association between demethylation of MAGE-A1 and response to taxan-based chemotherapy.

Response	No. of cases	No. of cases with demethylation of MAGE-A1 (%)	P-value[a]
CR	0	0 (0)	0.7245
PR	23	5 (21.7)	
NC	9	1 (11.1)	
PD	9	4 (44.4)	

MAGE-A1, melanoma-associated antigen-A1; CR, complete response; PR, partial response; NC, no change; PD, progressive disease. [a]Fisher's exact test (CR plus PR vs NC plus PD).

MAGE-A1 was demethylated in 4 MAGE-A1-positive GC cases, whereas the demethylation of MAGE-A1 was detected in 6 of the 37 MAGE-A1-negative cases (16.2%, P = 0.0021, Table IV). There was no clear association between the MAGE-A1 methylation status and the response to therapy in the group of 12 patients treated with paclitaxel alone, in the group of 29 patients treated with a combination of docetaxel and S-1, or in the total 41 patients (P=0.7245, Table V).

Effect of forced MAGE-A1 expression of GC cell line. As we detected a statistically significant association between MAGE-A1 expression and the response to taxan-based chemotherapy, we investigated the effect of forced MAGE-A1 expression on chemoresistance in a GC cell line, TMK-1. TMK-1 cells were stably transfected with a vector expressing MAGE-A1. TMK-1 cells were selected due to their low endogenous MAGE-A1 expression (data not shown). Clones were selected in G418 and examined for MAGE-A1 expression by Western blotting. Four clones that expressed MAGE-A1 at significantly higher levels than the empty vector-transfected cells were isolated (Fig. 2A). In order to determine the effect of MAGE-A1 expression on cell growth, we performed MTT assays. The rate of cell growth of the TMK-1 cells expressing higher levels of MAGE-A1 did not differ from that of the cells transfected with the empty vector up to day 2 (data not shown). We then examined the effect of MAGE-A1 expression on paclitaxel or docetaxel sensitivity. Contrary to our expectation, the IC_{50} levels for both paclitaxel and docetaxel in the MAGE-A1-transfected cells were lower than those of the empty vector-transfected cells (Fig. 2B). The mitomycin C IC_{50} levels did not differ significantly between the MAGE-A1-transfected cells and the empty vector-transfected cells.

Discussion

Previous data have suggested that the resistance to paclitaxel is associated with the increased expression of a variety of genes, including some that are localized near the cancer-testis genes (16). In the present study, we found that the expression of the protein encoded by the MAGE-A1 gene, which neighbors the cancer-testis antigen genes, was associated with the
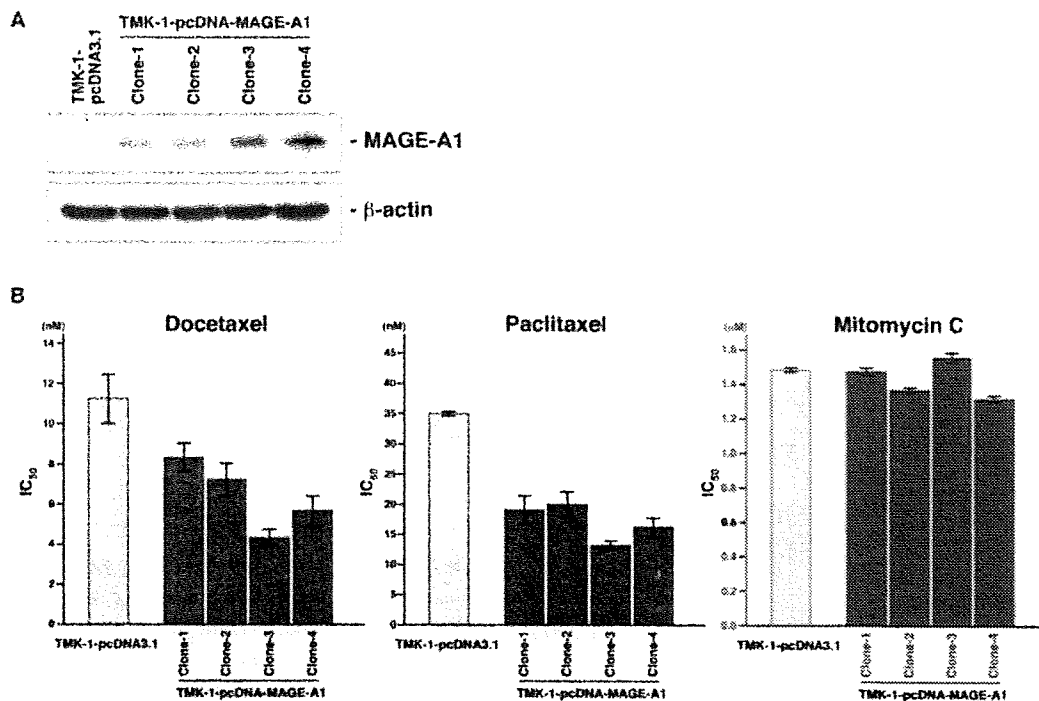
Figure 2. Effect of forced melanoma-associated antigen-A1 (MAGE-A1) expression on drug sensitivity. (A) Western blot analysis of the TMK-1 gastric cancer cell line stably transfected with the vector expressing MAGE-A1. Four G418-resistant clones overexpressing the MAGE-A1 protein, were isolated. (B) Drug sensitivity of MAGE-A1-transfected cells. MTT analysis revealed that forced MAGE-A1 expression increases the sensitivity to docetaxel and paclitaxel but does not change relative resistance to mitomycin C.

response of GC to taxan-based chemotherapy. All 4 patients with MAGE-A1-positive GC showed PD in response to paclitaxel or combination chemotherapy of docetaxel and S-1. These findings indicate that the expression of MAGE-A1 is a marker for the response to taxan-based chemotherapy. It is important to note that of the 29 patients treated with a combination of docetaxel and S-1, the response to chemotherapy could have been more influenced by S-1 than taxan. The influence of MAGE-A1 expression on the response to S-1 should be examined.

The cancer-specific expression of MAGE-A1 has been reported in several cancers including GC (26-28). It has been reported that the MAGE-A1 protein expression is associated with invasiveness, lymph node metastasis, advanced pathological stage, and poor prognosis (29). It has also been reported that the demethylation of both *MAGE-A1* and *MAGE-A3* occurs during the progressive stages of GC (19). In the present study, there was no clear association between MAGE-A1 expression/demethylation and the clinicopathological characteristics in the group of 20 GC cases obtained by resection. As we analyzed a limited number of GC samples, additional experiments are needed. *MAGE-A1* gene-encoded peptides are recognized by cytotoxic T lymphocytes (30), and clinical trials of cancer-specific immunotherapies against MAGE-A1-positive cells are underway. As taxan-based chemotherapies had no significant effects in the patients with MAGE-A1-positive GC in the present study, immunotherapy with antigen-presenting cells pulsed with MAGE-1 peptides could be an effective treatment for these patients.

DNA demethylation of the *MAGE-A1* gene was not associated with response to taxan-based chemotherapy. The hypermethylation of CpG islands is associated with the transcriptional silencing of several genes and has been proposed as a mechanism for the inactivation of tumor suppressor genes and tumor-related genes in human cancers (31). The identification of methylated genes could be useful for diagnosis and treatment of cancer and could provide insight into the process of carcinogenesis. In GC, several tumor suppressor and tumor-related genes have been shown to be inactivated by promoter hypermethylation (32,33), and DNA methylation increases with the progression of GC (34). Although the expression of MAGE-A1 was observed frequently in GCs with DNA demethylation of the *MAGE-A1* gene, we found 6 GC samples with *MAGE-A1* gene demethylation that did not express the MAGE-A1 protein. This result could be related to the extreme sensitivity of MSP, which can theoretically detect as few as 0.1% of cells with gene methylation (23). For the prediction of the response to the taxan-based chemotherapy, immunostaining could be a suitable method.

The biological function of MAGE proteins remains poorly understood. MAGE-A3 has been shown to bind *in vitro* to murine pro-caspase-12, thereby blocking the autoactivation of caspase-9 and the downstream activation of caspase-3 (35). The forced MAGE-A2 or MAGE-A6 expression in an ovarian cancer cell line induces the expression of the paclitaxel-resistant phenotype. These findings suggest that MAGE-A expression favors tumor cell survival and that MAGE-A proteins function as oncoproteins. In contrast, the

forced MAGE-A1 expression increased the sensitivity to paclitaxel and docetaxel in TMK-1 cells in the present study. This result suggests that MAGE-A1 does not participate directly in the drug-resistance phenotype despite the statistical association in the GC tissue samples. It has been reported that MAGE-A4 is commonly expressed in non-small cell lung cancers and has a proapoptotic effect and can function as a tumor suppressor protein (36), indicating that functional differences within the MAGE-A family may exist. Taken together, these results suggest that not all of the cancer-testis antigen genes participate directly in the taxol resistance. As the early activation of MAGE-A genes in cancer could be due to genomewide DNA hypomethylation, which is a frequently observed epigenetic event during carcinogenesis (37), the increased expression of genes which neighbor the *MAGE-A1* gene could contribute directly to the taxan-resistant phenotype. As we used the TMK-1 GC cell line only, the effect of forced MAGE-A1 expression on chemo-resistance in other GC cell lines should be investigated.

In conclusion, the results of the present retrospective study suggest that the expression of MAGE-A1 could be a marker for the prediction of resistance to taxan-based chemotherapy in patients with GC. As the rate of MAGE-A1-positive immunostaining was low in the present study, it is difficult to find a usefulness of MAGE-A1 in clinical application for the marker of the prediction of resistance to taxan-based chemotherapy in GC. A more sensitive marker is needed. A comprehensive analysis of expression of the cancer-testis antigen genes could reveal a more sensitive marker for the prediction of the response to taxan-based chemotherapy.

Acknowledgements

References

1. Yoshida K, Hirabayashi N, Takiyama W, *et al*: Phase I study of combination therapy with S-1 and docetaxel (TXT) for advanced or recurrent gastric cancer. Anticancer Res 24: 1843-1851, 2004.
2. Yoshida K, Ninomiya M, Takakura N, *et al*: Phase II study of docetaxel and S-1 combination therapy for advanced or recurrent gastric cancer. Clin Cancer Res 12: 3402-3407, 2006.
3. Ringel I and Horwitz SB: Studies with RP 56976 (taxotere): a semisynthetic analogue of taxol. J Natl Cancer Inst 83: 288-291, 1991.
4. Wada Y, Yoshida K, Suzuki T, *et al*: Synergistic effects of docetaxel and S-1 by modulating the expression of metabolic enzymes of 5-fluorouracil in human gastric cancer cell lines. Int J Cancer 119: 783-791, 2006.
5. Yasui W, Sentani K, Motoshita J and Nakayama H: Molecular pathobiology of gastric cancer. Scand J Surg 95: 225-231, 2006.
6. Ushijima T and Sasako M: Focus on gastric cancer. Cancer Cell 5: 121-125, 2004.
7. Yasui W, Oue N, Ito R, Kuraoka K and Nakayama H: Search for new biomarkers of gastric cancer through serial analysis of gene expression and its clinical implications. Cancer Sci 95: 385-392, 2004.
8. Oue N, Hamai Y, Mitani Y, *et al*: Gene expression profile of gastric carcinoma: identification of genes and tags potentially involved in invasion, metastasis, and carcinogenesis by serial analysis of gene expression. Cancer Res 64: 2397-2405, 2004.
9. Aung PP, Oue N, Mitani Y, *et al*: Systematic search for gastric cancer-specific genes based on SAGE data: melanoma inhibitory activity and matrix metalloproteinase-10 are novel prognostic factors in patients with gastric cancer. Oncogene 25: 2546-2557, 2006.
10. Duan Z, Feller AJ, Toh HC, Makastorsis T and Seiden MV: TRAG-3, a novel gene, isolated from a taxol-resistant ovarian carcinoma cell line. Gene 229: 75-81, 1999.
11. Feller AJ, Duan Z, Penson R, Toh HC and Seiden MV: TRAG-3, a novel cancer/testis antigen, is overexpressed in the majority of melanoma cell lines and malignant melanoma. Anticancer Res 20: 4147-4151, 2000.
12. Nimmrich I, Erdmann S, Melchers U, *et al*: Seven genes that are differentially transcribed in colorectal tumor cell lines. Cancer Lett 160: 37-43, 2000.
13. Chen Z, Zhu B and Wu Y: Expression of TRAG-3 antigen in non-small-cell lung carcinomas. Lung Cancer 38: 101-102, 2002.
14. Wu YZ, Zhao TT, Ni B, Zou LY, Liu HL and Zhu B: Expression of TRAG-3 in breast cancer. Int J Cancer 107: 167-168, 2003.
15. Zhu B, Chen Z, Cheng X, *et al*: Identification of HLA-A*0201-restricted cytotoxic T lymphocyte epitope from TRAG-3 antigen. Clin Cancer Res 9: 1850-1857, 2003.
16. Duan Z, Duan Y, Lamendola DE, *et al*: Overexpression of MAGE/GAGE genes in paclitaxel/doxorubicin-resistant human cancer cell lines. Clin Cancer Res 9: 2778-2785, 2003.
17. Miyagawa N, Kono K, Mimura K, Omata H, Sugai H and Fujii H: A newly identified MAGE-3-derived, HLA-A24-restricted peptide is naturally processed and presented as a CTL epitope on MAGE-3-expressing gastrointestinal cancer cells. Oncology 70: 54-62, 2006.
18. Scanlan MJ, Gure AO, Jungbluth AA, Old LJ and Chen YT: Cancer/testis antigens: an expanding family of targets for cancer immunotherapy. Immunol Rev 188: 22-32, 2002.
19. Honda T, Tamura G, Waki T, *et al*: Demethylation of MAGE promoters during gastric cancer progression. Br J Cancer 90: 838-843, 2004.
20. Lauren P: The two histological main types of gastric carcinoma. Diffuse and so-called intestinal type carcinoma: an attempt at histological classification. APMIS 64: 31-49, 1965.
21. TNM classification of malignant tumors. Sobin LH and Wittekind CH (eds). 6th edition. John Wiley & Sons, New York, pp65-68, 2002.
22. Rimoldi D, Salvi S, Reed D, *et al*: cDNA and protein characterization of human MAGE-10. Int J Cancer 82: 901-907, 1999.
23. Herman JG, Graff JR, Myohanen S, Nelkin BD and Baylin SB: Methylation-specific PCR: a novel PCR assay for methylation status of CpG islands. Proc Natl Acad Sci USA 93: 9821-9826, 1996.
24. Ochiai A, Yasui W and Tahara E: Growth-promoting effect of gastrin on human gastric carcinoma cell line TMK-1. Jpn J Cancer Res 76: 1064-1071, 1985.
25. Yasui W, Ayhan A, Kitadai Y, *et al*: Increased expression of p34cdc2 and its kinase activity in human gastric and colonic carcinomas. Int J Cancer 53: 36-41, 1993.
26. Inoue H, Li J, Honda M, *et al*: MAGE-1 mRNA expression in gastric carcinoma. Int J Cancer 64: 76-77, 1995.
27. Mori M, Inoue H, Mimori K, *et al*: Expression of MAGE genes in human colorectal carcinoma. Ann Surg 224: 183-188, 1996.
28. Utsunomiya T, Inoue H, Tanaka F, *et al*: Expression of cancer-testis antigen (CTA) genes in intrahepatic cholangiocarcinoma. Ann Surg Oncol 11: 934-940, 2004.
29. Jung EJ, Kim MA, Lee HS, *et al*: Expression of family A melanoma antigen in human gastric carcinoma. Anticancer Res 25: 2105-2111, 2005.
30. Fujie T, Tahara K, Tanaka F, Mori M, Takesako K and Akiyoshi T: A MAGE-1-encoded HLA-A24-binding synthetic peptide induces specific anti-tumor cytotoxic T lymphocytes. Int J Cancer 80: 169-172, 1999.
31. Jones PA and Baylin SB: The fundamental role of epigenetic events in cancer. Nat Rev Genet 3: 415-428, 2002.

32. Oue N, Motoshita J, Yokozaki H, *et al*: Distinct promoter hypermethylation of p16INK4a, CDH1, and RAR-beta in intestinal, diffuse-adherent, and diffuse-scattered type gastric carcinomas. J Pathol 198: 55-59, 2002.
33. Shutoh M, Oue N, Aung PP, *et al*: DNA methylation of genes linked with retinoid signaling in gastric carcinoma: expression of the retinoid acid receptor beta, cellular retinol-binding protein 1, and tazarotene-induced gene 1 genes is associated with DNA methylation. Cancer 104: 1609-1619, 2005.
34. Oue N, Mitani Y, Motoshita J, *et al*: Accumulation of DNA methylation is associated with tumor stage in gastric cancer. Cancer 106: 1250-1259, 2006.
35. Morishima N, Nakanishi K, Takenouchi H, Shibata T and Yasuhiko Y: An endoplasmic reticulum stress-specific caspase cascade in apoptosis. Cytochrome c-independent activation of caspase-9 by caspase-12. J Biol Chem 277: 34287-34294, 2002.
36. Peikert T, Specks U, Farver C, Erzurum SC and Comhair SA: Melanoma antigen A4 is expressed in non-small cell lung cancers and promotes apoptosis. Cancer Res 66: 4693-4700, 2006.
37. Ehrlich M: DNA methylation in cancer: too much, but also too little. Oncogene 21: 5400-5413, 2002.

Activation of KIF4A as a Prognostic Biomarker and Therapeutic Target for Lung Cancer

Masaya Taniwaki,[1,2] Atsushi Takano,[1] Nobuhisa Ishikawa,[1] Wataru Yasui,[3] Kouki Inai,[4] Hitoshi Nishimura,[5] Eiju Tsuchiya,[6] Nobuoki Kohno,[2] Yusuke Nakamura,[1] and Yataro Daigo[1]

Abstract   **Purpose and Experimental Design:** To identify molecules that might be useful as diagnostic/prognostic biomarkers and as targets for the development of new molecular therapies, we screened genes that were highly transactivated in a large proportion of 101 lung cancers by means of a cDNA microarray representing 27,648 genes. We found a gene encoding KIF4A, a kinesin family member 4A, as one of such candidates. Tumor tissue microarray was applied to examine the expression of KIF4A protein and its clinicopathologic significance in archival non–small cell lung cancer (NSCLC) samples from 357 patients. A role of KIF4A in cancer cell growth and/or survival was examined by small interfering RNA experiments. Cellular invasive activity of KIF4A on mammalian cells was examined using Matrigel assays.
Results: Immunohistochemical staining detected positive KIF4A staining in 127 (36%) of 357 NSCLCs and 19 (66%) of 29 small-cell lung cancers examined. Positive immunostaining of KIF4A protein was associated with male gender ($P = 0.0287$), nonadenocarcinoma histology ($P = 0.0097$), and shorter survival for patients with NSCLC ($P = 0.0005$), and multivariate analysis confirmed its independent prognostic value ($P = 0.0012$). Treatment of lung cancer cells with small interfering RNAs for *KIF4A* suppressed growth of the cancer cells. Furthermore, we found that induction of exogenous expression of KIF4A conferred cellular invasive activity on mammalian cells.
Conclusions: These data strongly implied that targeting the KIF4A molecule might hold a promise for the development of anticancer drugs and cancer vaccines as well as a prognostic biomarker in clinic.

Lung cancer is one of the most common and fatal cancers in the world (1). A number of genetic alterations associated with development and progression of lung cancer have been reported; however, its molecular mechanisms still largely remain unclear (2). Two major histologically distinct types of lung cancer, non–small cell lung cancer (NSCLC) and small-cell lung cancer (SCLC) have different pathophysiologic and clinical features that suggest differences in the mechanisms of their carcinogenesis. NSCLC accounts for nearly 80% of lung cancers, whereas SCLC accounts for 20% of them and is

categorized as neuroendocrine tumors of the lung with certain morphologic, ultrastructural, and immunohistochemical characteristics (3, 4). In spite of applying surgical techniques combined with various treatment modalities such as radiotherapy and chemotherapy, the overall 5-year survival rate of lung cancer is still low at ~15% (5). Patients with SCLC respond favorably to the first-line multiagent chemotherapy; however, they often relapse in a short time. Hence, the only 20% of patients with limited-stage disease can be cured with combined modality therapy and <5% of those with extensive disease are able to achieve 5-year survival after the initial diagnosis (6, 7). Therefore, new therapeutic strategies focusing on SCLC as well as NSCLC such as molecular-targeted agents are eagerly awaited.

The genome-wide cDNA microarray analysis covering complete or near-complete set of genes enabled us to obtain comprehensive gene expression profiles and to compare the gene expression levels with clinicopathologic and biological information of cancers (8–14). This kind of approach is also useful to identify unknown molecules involved in the carcinogenic pathway. Through the gene expression profile analysis of 15 SCLCs and 86 NSCLCs coupled with purification of cancer cell population by laser microdissection on a cDNA microarray consisting of 27,648 genes, and their comparison with the expression profile data of 31 normal human tissues (27 adult and 4 fetal organs; refs. 15, 16), we identified a number of potential molecular targets for diagnosis, treatment,

and/or choice of therapy (8–12). To verify the biological and clinicopathologic significance of the respective gene products, we have also been performing high-throughput screening of loss-of-function effects by means of the RNA interference technique as well as tumor tissue microarray analysis of clinical lung cancer materials (17–30). This systematic approach revealed that kinesin family member 4A (KIF4A) was frequently overexpressed in the great majority of lung cancers and was essential to growth or progression of lung cancers.

Kinesin superfamily proteins, such as KIF4A, are microtubule-based motor proteins that generate directional movement along microtubules. KIFs are key players or central proteins in the intracellular transport system, which is essential for cellular function and morphology, including cell division (31). The kinesin superfamily is also the first large protein family in mammals whose constituents have been completely identified and confirmed both *in silico* and *in vivo* (32). A large portion of human KIF4A is associated with the nuclear matrix during the interphase, whereas a small portion of them is found in the cytoplasm. During mitosis, it is associated with chromosomes throughout the entire process (33). A previous microarray study disclosed the elevated expression of *KIF4A* mRNA in human cervical cancer (34), although no report has clarified the significance of KIF4A transactivation in human cancer progression and its potential as a therapeutic target.

We here report the identification of KIF4A to be a promising target as a prognostic biomarker as well as for development of therapeutic agents and cancer vaccines, and also describe possible biological roles of KIF4A protein in progression of lung cancer.

Materials and Methods

Lung cancer cell lines and tissue samples. The human lung cancer cell lines used in this study were as follows: lung adenocarcinomas A427, A549, LC319, and NCI-H1373; lung squamous cell carcinomas (SCC) RERF-LC-AI, SK-MES-1, NCI-H226, NCI-H520, and NCI-H2170; and SCLCs DMS114, DMS273, SBC-3, and SBC-5. All cells were grown in monolayers in appropriate medium supplemented with 10% FCS and were maintained at 37°C in atmospheres of humidified air with 5% CO_2. Human small airway epithelial cells were grown in optimized medium purchased from Cambrex Bio Science, Inc. Primary lung cancer tissue samples had been obtained with informed consent as described previously (8, 12). A total of 357 NSCLCs and adjacent normal lung tissue samples for immunostaining on tissue microarray were also obtained from Saitama Cancer Center (Saitama, Japan). These patients received resection of their primary cancers, and among them only patients with positive lymph node metastasis were treated with cisplatin-based adjuvant chemotherapies after their surgery. Twenty-nine SCLC samples obtained from Hiroshima University (Hiroshima, Japan) and Saitama Cancer Center were also used in this study. This study and the use of all clinical materials were approved by individual institutional ethical committees.

Semiquantitative reverse transcription-PCR. Total RNA was extracted from cultured cells using the TRIzol reagent (Life Technologies, Inc.) according to the manufacturer's protocol. Extracted RNAs were treated with DNase I (Nippon Gene) and reversely transcribed using oligo(dT) primer and SuperScript II. Semiquantitative reverse transcription-PCR (RT-PCR) experiments were carried out with the following synthesized *KIF4A*-specific primers or with β-actin (*ACTB*)–specific primers as an internal control: *KIF4A*, 5'-CAAAAACCAGCTTCTTCTCTGG-3' and 5'-CAGGAAAGATCACAACCTCATTC-3'; *ACTB*, 5'-GAGGTGAT-AGCATTGCTTTCG-3' and 5'-CAAGTCAGTGTACAGGTAAGC-3'. PCR

reactions were optimized for the number of cycles to ensure product intensity within the logarithmic phase of amplification.

Northern blot analysis. Human multiple-tissue blots (BD Biosciences Clontech) were hybridized with a ^{32}P-labeled PCR product of *KIF4A*. The cDNA probe of KIF4A was prepared by RT-PCR using the primers described above. Prehybridization, hybridization, and washing were done according to the supplier's recommendations. The blots were autoradiographed at room temperature for 30 h with intensifying BAS screens (Bio-Rad).

Western blotting. Cells were lysed in lysis buffer: 50 mmol/L Tris-HCl (pH 8.0), 150 mmol/L NaCl, 0.5% NP40, 0.5% deoxycholate-Na, 0.1% SDS, plus protease inhibitor (Protease Inhibitor Cocktail Set III; Calbiochem/Merck KGaA). We used an enhanced chemiluminescence Western blotting analysis system (GE Healthcare Biosciences), as previously described (19, 20). A commercially available goat polyclonal anti-KIF4A antibody was purchased from Abcam, Inc., and was proved to be specific to human KIF4A, by Western blot analysis using lysates of lung cancer cell lines.

Immunocytochemistry. Cultured cells were washed twice with PBS(-), fixed in 4% formaldehyde solution for 30 min at 37°C, and rendered permeable by treatment for 3 min with PBS(-) containing 0.1% Triton X-100. Cells were covered with CAS-BLOCK (Zymed) for 7 min to block nonspecific binding before the primary antibody reaction. Then, the cells were incubated with polyclonal antibody to human KIF4A protein (Abcam). The immunocomplexes were stained with a donkey anti-goat secondary antibody conjugated to Alexa 488 (Molecular Probes) and viewed with a laser confocal microscope (TCS SP2 AOBS: Leica Microsystems).

Immunohistochemistry and tissue microarray analysis. To investigate the significance of KIF4A overexpression in clinical lung cancers, we stained tissue sections using ENVISION+ kit/horseradish peroxidase (DakoCytomation). Anti-KIF4A antibody (Abcam) was added after blocking of endogenous peroxidase and proteins, and each section was incubated with horseradish peroxidase–labeled anti-goat IgG as the secondary antibody. Substrate chromogen was added and the specimens were counterstained with hematoxylin. Tumor tissue microarrays were constructed as published previously, using formalin-fixed NSCLCs (35–37). Tissue areas for sampling were selected based on visual alignment with the corresponding H&E-stained sections on slides. Three, four, or five tissue cores (diameter 0.6 mm; height 3-4 mm) taken from donor-tumor blocks were placed into recipient paraffin blocks using a tissue microarrayer (Beecher Instruments). A core of normal tissue was punched from each case. Five-micrometer sections of the resulting microarray block were used for immunohistochemical analysis. Positivity for KIF4A was assessed semiquantitatively by three independent investigators without prior knowledge of the clinical follow-up data, each of whom recorded staining intensity as either negative (no appreciable staining in tumor cells) or positive (brown staining appreciable in the nucleus and cytoplasm of tumor cells). Cases were accepted as positive only if reviewers independently defined them as such.

Statistical analysis. Statistical analyses were done using the StatView statistical program (SaS). We used contingency tables to analyze the relationship between KIF4A expression and clinicopathologic variables in NSCLC patients. Tumor-specific survival curves were calculated from the date of surgery to the time of death related to NSCLC, or to the last follow-up observation. Kaplan-Meier curves were calculated for each relevant variable and for KIF4A expression; differences in survival times among patient subgroups were analyzed using the log-rank test. Univariate and multivariate analyses were done with the Cox proportional hazard regression model to determine associations between clinicopathologic variables and cancer-related mortality. First, we analyzed associations between death and possible prognostic factors, including age, gender, histologic type, pT classification, pN classification, and smoking history, taking into consideration one factor at a time. Second, multivariate Cox analysis was applied on backward (stepwise) procedures that always forced KIF4A expression into the

model, along with any and all variables that satisfied an entry level of $P < 0.05$. As the model continued to add factors, independent factors did not exceed an exit level of $P < 0.05$.

RNA interference assay. We had previously established a vector-based RNA interference system, psiH1BX3.0, that was designed to synthesize small interfering RNAs (siRNA) in mammalian cells (17–27, 29, 30). Ten micrograms of siRNA expression vector were transfected using 30 μL of LipofectAMINE 2000 (Invitrogen) into lung cancer cell lines SBC-3, SBC-5, LC319, and A549. The transfected cells were cultured for 7 days in the presence of appropriate concentrations of geneticin (G418); the number of colonies was counted by Giemsa staining; and viability of cells was evaluated by 3-(4,5-dimethylthiazol-2-yl)-2,5-diphenyltetrazolium bromide assay at 7 days after the treatment. Briefly, cell counting kit-8 solution (Dojindo) was added to each dish at a concentration of 1/10 volume, and the plates were incubated at 37°C for additional 2 h. Absorbance was then measured at 490 nm, and at 630 nm as a reference, with a Microplate Reader 550 (Bio-Rad). To confirm suppression of *KIF4A* mRNA expression, semiquantitative RT-PCR experiments were carried out with the following synthesized *KIF4A*-specific primers according to the standard protocol. The target sequences of the synthetic oligonucleotides for RNA interference were as follows: control 1 (luciferase/LUC: *Photinus pyralis* luciferase gene), 5'-CGTACGCGGAATACTTCGA-3'; control 2 (scramble/SCR: *chloroplast Euglena gracilis* gene coding for 5S and 16S rRNAs), 5'-GCGCGCTTTGTAGGATTCG-3'; siRNA-*KIF4A*-1, 5'-GGAAGAATTGGTTCTTGAA-3'; siRNA-*KIF4A*-2, 5'-GATGTGGCT-CAACTCAAAG-3'.

Matrigel invasion assay. We cloned the entire coding sequence into the appropriate site of p3XFLAG-CMV-10 plasmid vector (Sigma). COS-7 and NIH3T3 cells transfected either with plasmids expressing KIF4A or with mock plasmids were grown to near confluence in DMEM containing 10% FCS. The cells were harvested by trypsinization, washed in DMEM without addition of serum or proteinase inhibitor, and suspended in DMEM at 5×10^5/mL. Before preparing the cell suspension, the dried layer of Matrigel matrix (Becton Dickinson Labware) was rehydrated with DMEM for 2 h at room temperature. DMEM (0.75 mL) containing 10% FCS was added to each lower chamber in 24-well Matrigel invasion chambers, and 0.5 mL (2.5×10^5 cells) of cell suspension were added to each insert of the upper chamber. The plates of inserts were incubated for 22 h at 37°C. After incubation, the chambers were processed; cells invading through the Matrigel were fixed and stained by Giemsa as directed by the supplier (Becton Dickinson Labware).

Results

Expression of KIF4A in lung cancers and normal tissues. Using a cDNA microarray to screen for genes that were highly transactivated in a large proportion of lung cancers, we identified *KIF4A* gene as a good candidate. This gene showed a 5-fold or higher level of expression in the majority of SCLC cases and in ~40% of NSCLCs we examined. Subsequently, we confirmed its transactivation by semiquantitative RT-PCR experiments in all of eight SCLC cases and in 5 of 10 NSCLC cases (Fig. 1A). We further confirmed a high level of KIF4A in 10 of 12 lung cancer cell lines by semiquantitative RT-PCR and Western blot analyses using anti-KIF4A antibody (Fig. 1B, *top* and *bottom*). To determine the subcellular localization of endogenous KIF4A in lung cancer cells, we did immunocyto-chemical analysis using anti-KIF4A polyclonal antibodies; KIF4A protein was localized in the cytoplasm and nucleus of DMS273 cells (Fig. 1C).

Northern blot analysis using *KIF4A* cDNA as a probe identified a 5.0-kb transcript specifically in testis among the 23 normal human tissues examined (Fig. 1D). Furthermore, we

compared KIF4A protein expressions in five normal tissues (liver heart, kidney, lung, and testis) with those in lung cancers using anti-KIF4A polyclonal antibodies by immunohisto-chemistry. KIF4A expressed abundantly in testis (mainly in cytoplasm and/or nucleus of primary spermatocytes) and lung cancers; however, its expression was hardly detectable in the remaining four normal tissues (Fig. 2A).

Association of KIF4A overexpression with poor prognosis of NSCLC. In SCLC and NSCLC tissues, immunohistochemical analysis with anti-KIF4A polyclonal antibodies showed that KIF4A localized in the cytoplasm and nucleus (Fig. 2B). Interestingly, the invasive border of the tumor adjacent to the noncancerous areas showed the tendency of stronger staining. Using tissue microarrays prepared from 357 NSCLCs and 29 SCLCs, we did immunohistochemical analysis with anti-KIF4A polyclonal antibodies and found positive staining in 127 (36%) of the 357 NSCLC cases and 19 (66%) of the 29 SCLCs (Fig. 2C), whereas no staining was observed in any of corresponding normal lung tissues examined. Of these KIF4A-positive NSCLC cases, 68 were adenocarcinomas (30% of 223), 37 were SCCs (39% of 94 cases), 14 were LCCs (52% of 27 cases), and 8 were adenosquamous cell carcinomas (62% of 13). We then examined correlations of the KIF4A expression in surgically resected NSCLCs with various clinicopathologic variables. The sample size of SCLCs was too small to be evaluated further. Statistical analysis revealed that gender (higher in male; $P = 0.0287$ by χ^2 test) and histology (higher in nonadenocarcinomas; $P = 0.0097$ by χ^2 test) were significantly associated with the KIF4A positivity (Table 1). The Kaplan-Meier method indicated significant association between KIF4A status (positive versus negative) in NSCLCs and tumor-specific survival rate (shorter survival periods in KIF4A-positive cases; $P = 0.0005$ by the log-rank test; Fig. 2D, *left*). Positive immunostaining of KIF4A protein was associated with shorter survival for patients with lung adenocarcinoma ($P = 0.005$ by the log-rank test), whereas KIF4A expression also tended to be an unfavorable prognostic factor for patients with lung SCC or LCC ($P = 0.05$ by the log-rank test; Supplementary Figs. S1, *left* and *right*). By univariate analysis, histology (adenocarcinomas versus nonadenocarcinomas), tumor size (pT_1 versus pT_{2-4}), lymph node metastasis (pN_0 versus pN_{1-3}), age (<65 years versus ≥65 years), gender (female versus male), and KIF4A positivity (negative versus positive) were all significantly related to poor tumor-specific survival of NSCLC patients (Table 2). Furthermore, multivariate analysis using the Cox proportional hazard model indicated that pT stage, pN stage, age, and positive KIF4A staining were independent prognostic factors for NSCLC (Table 2). To further analyze the prognostic value of KIF4A in more homogeneous populations of patients, we validated the relationship between KIF4A expression and survival by subgroup analysis based on tumor stage and the status of adjuvant treatment. We divided the 357 NSCLC cases into two subgroups with or without the adjuvant therapy: group 1 for node-negative cases (pN_0; 212 patients) who had no adjuvant treatment and group 2 for node-positive cases (pN_{1-3}; 145 patients) who were treated with cisplatin-based adjuvant chemotherapy after surgery. We confirmed that KIF4A expression was significantly associated with poor prognosis in the group 1 patients ($P = 0.03$ by the log-rank test; Fig. 2D, *middle*), as well as with that in the group 2 patients ($P = 0.003$ by the log-rank test; Fig. 2D, *right*).

A

Clinical SCLC

| K6 | K24 | K45 | K46 | K64 | K76 | K81 | K95 | Normal lung |

KIF4A

ACTB

Clinical NSCLC

ADC | SCC | Normal lung

9 10 13 14 40 8 18 19 20 44

KIF4A

ACTB

B

NSCLC cell line SCLC cell line Airway epithelia

A427 A549 H1373 H226 H520 H2170 SK-MES-1 RERF-LC-AI DMS114 DMS273 SBC3 SBC5 SAEC

KIF4A

ACTB

NSCLC cell line SCLC cell line Airway epithelia

(kDa) A427 A549 H1373 H226 H520 H2170 SK-MES-1 RERF-LC-AI DMS114 DMS273 SBC3 SBC5 SAEC

250 —

150 —

100 — IB: anti-KIF4A
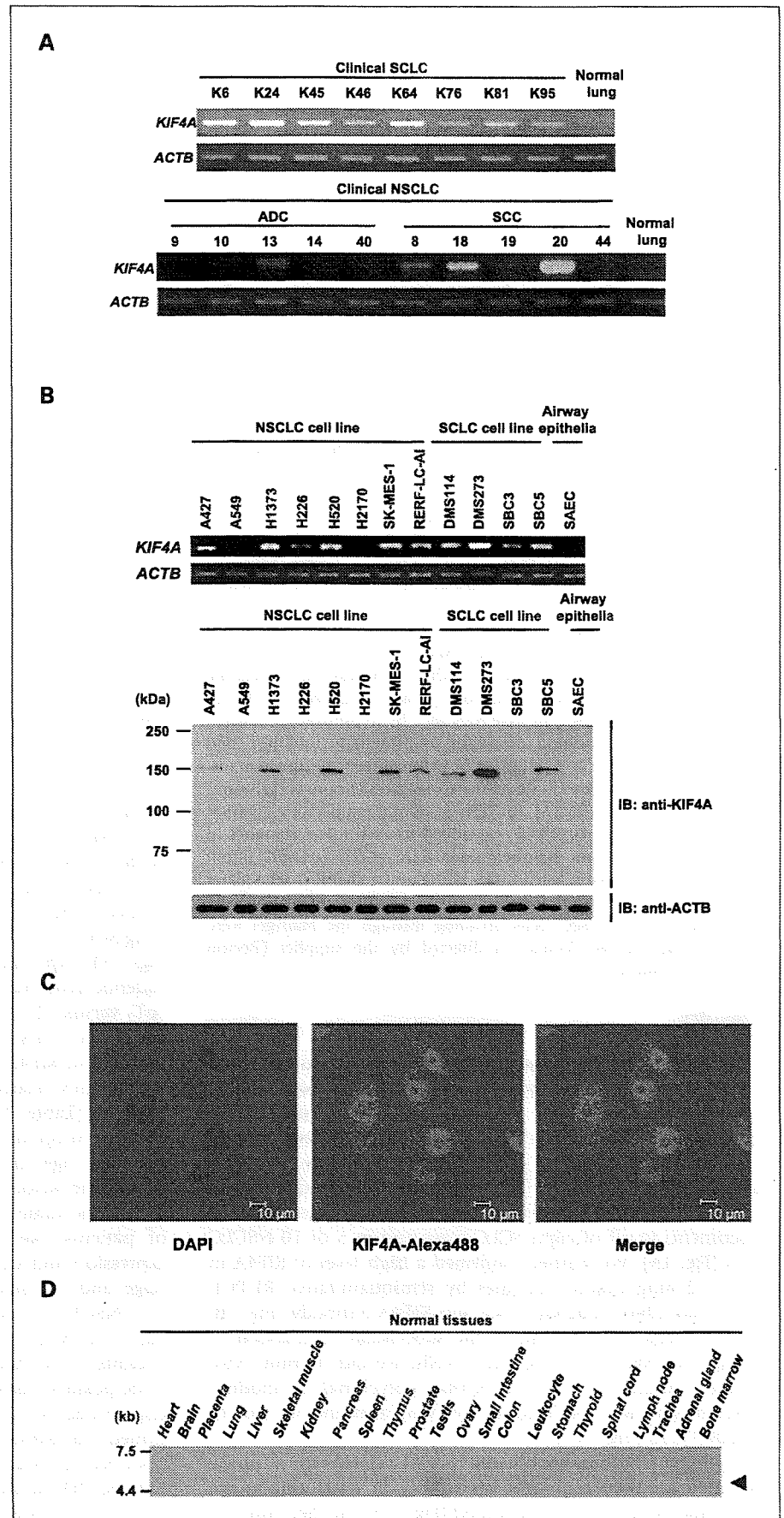
75 —

IB: anti-ACTB

Fig. 1. KIF4A expression in lung cancers and normal tissues. *A*, expression of *KIF4A* in clinical samples of SCLC (*top panels*) and NSCLC (*bottom panels*), and normal lung tissues, analyzed by semiquantitative RT-PCR. We prepared appropriate dilutions of each single-stranded cDNA prepared from mRNAs of lung cancer samples, using the level of β-actin (*ACTB*) expression as a quantitative control. *B*, expression of KIF4A in lung cancer cell lines, examined by semiquantitative RT-PCR (*top panels*) and Western blot analyses (*bottom panels*). IB, immunoblot. Expression of ACTB served as a quantity control. *C*, subcellular localization of endogenous KIF4A protein in DMS273 cells. KIF4A staining is observed at the cytoplasm and nucleus of the cells. DAPI, 4′,6-diamidino-2-phenylindole. *D*, expression of *KIF4A* in normal human tissues, detected by Northern blot analysis.

C

DAPI KIF4A-Alexa488 Merge

D

Normal tissues

Heart Brain Placenta Lung Liver Skeletal muscle Kidney Pancreas Spleen Thymus Prostate Testis Ovary Small intestine Colon Leukocyte Stomach Thyroid Spinal cord Lymph node Trachea Adrenal gland Bone marrow

(kb)

7.5 —

4.4 —

−652−

Inhibition of growth of lung cancer cells by siRNA against KIF4A. To assess whether KIF4A is essential for growth or survival of lung cancer cells, we constructed plasmids to express siRNAs against KIF4A (si-*KIF4A*s) as well as control plasmids (siRNAs for luciferase and scramble) and transfected them into

SBC-3, SBC-5, and LC319 cells, which strongly expressed *KIF4A* (Fig. 3; Supplementary Fig. S2). The *KIF4A*-mRNA levels in cells transfected with si-*KIF4A*-1 or si-*KIF4A*-2 were significantly decreased in comparison with cells transfected with either control siRNAs (Fig. 3A; Supplementary Fig. S2). We observed
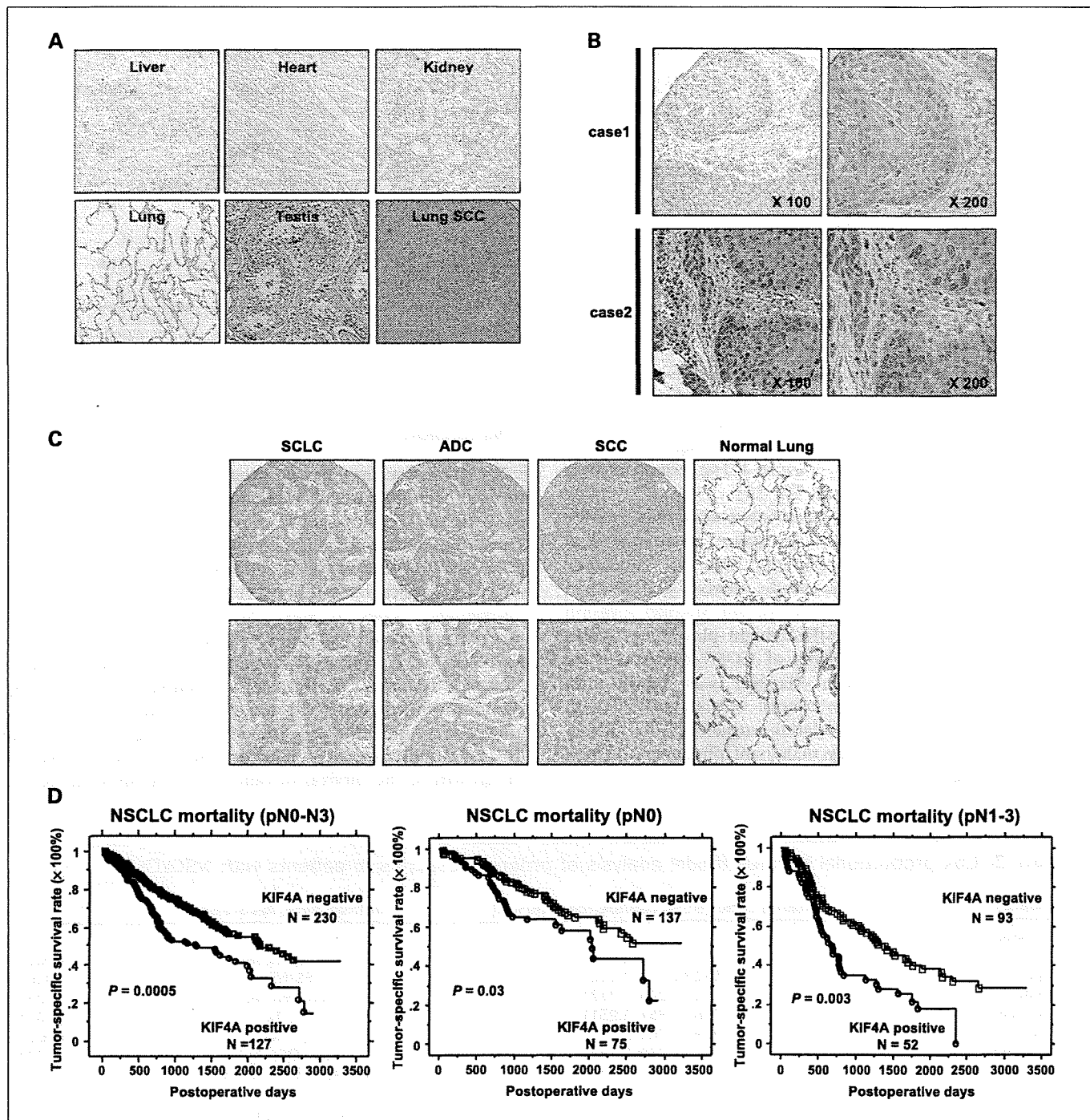

Fig. 2. Immunohistochemical and clinicopathologic evaluation of KIF4A protein expression in lung cancer tissues. *A*, expression of KIF4A in five normal human tissues as well as lung SCC, detected by immunohistochemical staining. Magnification, ×100. Positive staining appeared predominantly in the cytoplasm and nucleus of primary spermatocytes in the testis and lung cancer cells. *B*, expression of KIF4A in lung SCC, detected by immunohistochemical staining. Magnifications, ×100 (*left*) and ×200 (*right*). Invasive border of the tumor adjacent area to the noncancerous area showed the tendency of stronger staining. *C*, KIF4A expression in SCLCs, lung adenocarcinomas (*ADC*), and lung SCCs. Its expression is not observed in normal lung. *D*, association of KIF4A overexpression with poor clinical outcomes for NSCLC patients. Left, Kaplan-Meier analysis of tumor-specific survival in patients with NSCLC according to KIF4A expression. Middle, Kaplan-Meier analysis of tumor-specific survival period among group 1 patients with node-negative (pN0) NSCLC according to presence or absence of KIF4A. Right, Kaplan-Meier analysis of tumor-specific survival period among group 2 patients with node-positive (pN$_{1-3}$) tumor according to presence or absence of KIF4A.

—653—

Table 1. Association between KIF4A positivity in NSCLC tissues and patient characteristics

	Total (n = 357)	KIF4A positive (n = 127)	KIF4A absent (n = 230)	χ^2	P (positive vs absent)
Gender					
Female	107	29	78	4.784	0.0287*
Male	250	98	152		
Age (y)					
<65	177	69	108	1.78	NS
≥65	180	58	122		
Histologic type					
ADC	223	68	155	6.692	0.0097*
Non-ADC	134	59	75		
pT factor					
T_1	113	36	77	0.996	NS
T_{2-4}	244	91	153		
pN factor					
N_0	212	75	137	0.009	NS
N_{1-3}	145	52			
Smoking history					
Never smoker	104	32	72	1.478	NS
Smoker	253	95	158		

Abbreviations: ADC, adenocarcinoma; non-ADC, SCC plus large cell carcinoma and adenosquamous cell carcinoma; NS, no significance.
*P < 0.05 (χ^2 test).

significant decreases in the numbers of viable cells (Figs. 3B-C; Supplementary Fig. S2). si-*KIF4A*s revealed no significant effect on cell viability of A549 cells in which KIF4A expression was hardly detectable (Supplementary Fig. S3).

Cellular invasive effect of KIF4A on mammalian cells. As the immunohistochemical analysis on tissue microarray had indicated that lung cancer patients with KIF4A-positive tumors revealed shorter cancer-specific survival periods than those with KIF4A-negative tumors, we did Matrigel invasion assays to determine whether KIF4A might play some role in cellular invasive ability. Invasion of COS-7-KIF4A cells or NIH3T3-KIF4A cells through Matrigel was significantly enhanced, compared with the control cells transfected with mock plasmids, thus independently suggesting that KIF4A could contribute to the highly malignant phenotype of lung cancer cells (Fig. 4A-C).

Discussion

Several molecular-targeting drugs have been developed and proved their efficacy in cancer therapy; however, the proportion of patients showing good response is still limited (38). Therefore, further development of molecular-targeting drugs for cancer is urgently awaited. We have screened the therapeutic target molecules by the following strategy: (a) identifying up-regulated genes in lung cancer by genome-wide cDNA microarray system (8-12); (b) verifying the candidate genes for its no, or very low level of, expression in normal tissues by Northern blotting (15, 16); (c) validating clinicopathologic significance of their overexpression by means of tissue micro-array containing hundreds of archived lung cancer samples (18-30); and (d) verifying whether the target gene is essential for growth or the survival of cancer cells by RNA interference

Table 2. Cox proportional hazards model analysis of prognostic factors in patients with NSCLCs

| Variables	Hazards ratio (95% confidence interval)	Unfavorable/favorable	P
Univariate analysis			
KIF4A	1.690 (1.254-2.276)	Positive/negative	0.0006*
Age (y)	1.572 (1.171-2.112)	≥65/65>	0.0026*
Gender	1.690 (1.203-2.372)	Male/female	0.0025*
pT factor	2.708 (1.857-3.951)	T_{2-4}/T_1	<0.0001*
pN factor	2.369 (1.769-3.171)	N_{1-3}/N_0	<0.0001*
Histologic type	1.407 (1.050-1.884)	Non-ADC/ADC	0.0222*
Smoking history	1.193 (0.862-1.652)	Smoker/never smoker	NS
Multivariate analysis			
KIF4A	1.657 (1.221-2.248)	Positive/negative	0.0012*
Age (y)	1.754 (1.300-2.365)	≥65/65>	0.0002*
Gender	1.368 (0.942-1.986)	Male/female	NS
pT factor	2.130 (1.446-3.138)	T_{2-4}/T_1	0.0001*
pN factor	2.429 (1.800-3.279)	N_{1-3}/N_0	<0.0001*
Histologic type	0.99 (0.717-1.367)	Non-ADC/ADC	NS

*P < 0.05.
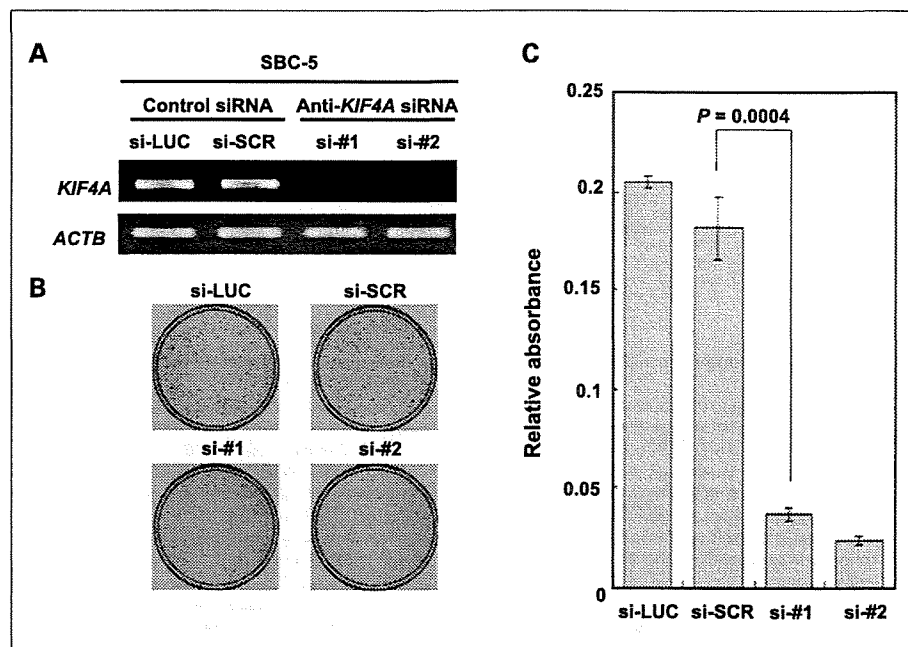
Fig. 3. Inhibition of growth of lung cancer cells that overexpressed *KIF4A* by siRNA against *KIF4A*. *A*, expression of *KIF4A* in response to si-*KIF4A* (*si-#1* or *si-#2*) or control siRNAs (LUC or SCR) in SBC-5 cells, analyzed by semiquantitative RT-PCR. *B*, colony formation assays of SBC-5 cells transfected with specific siRNAs or control plasmids. *C*, viability of SBC-5 cells evaluated by 3-(4,5-dimethylthiazol-2-yl)-2,5-diphenyltetrazolium bromide assay in response to si-*KIF4A* (*si-#1* or *si-#2*), si-LUC, or si-SCR. All assays were done thrice, and in triplicate wells.

assay (17, 19, 20, 22–27, 29, 30). Using this approach, we have shown here that KIF4A is frequently overexpressed in clinical lung cancer samples and cell lines, and that its gene products play indispensable roles in the growth and progression of lung cancer cells.

Kinesins constitute a superfamily of microtubule-based motor proteins with 45 members in mice and humans that represent diverse functions, including the transport of vesicles, organelles, chromosomes, protein complexes, and mRNA (39–42). The inhibition of the mitotic kinesin Eg5 by small molecules such as monastrol is being evaluated as an approach to develop a novel class of antiproliferative drugs for the treatment of malignant tumors (43, 44). The KIF4 subfamily consists of KIF4A, KIF4B, KIF21A, and KIF21B (39). KIF4A is a novel component of the chromosome condensation and segregation machinery functioning in multiple steps of mitotic division and plays essential roles in regulating anaphase spindle dynamics and the completion of cytokinesis (45, 46). KIF4 is

also shown to be involved in neuronal survival (40). In this study, the treatment of NSCLC cells with specific siRNA to knockdown *KIF4A* expression resulted in suppression of cancer cell growth. We also showed additional evidences supporting the significance of this pathway in carcinogenesis; for example, the expression of KIF4A also resulted in the significant promotion of the cellular invasion in *in vitro* assays. Moreover, clinicopathologic evidence obtained through our tissue microarray experiments indicated that NSCLC patients with KIF4A-positive tumors had shorter cancer-specific survival periods than those with KIF4A-negative tumors. The results obtained by *in vitro* and *in vivo* assays strongly suggested that KIF4A is likely to be an important growth factor and might be associated with a highly malignant phenotype of lung cancer cells, although the molecular mechanisms underlying increased KIF4A expression levels in many cancer cells remains to be clarified. Because KIF4A should be classified as one of the typical cancer testis

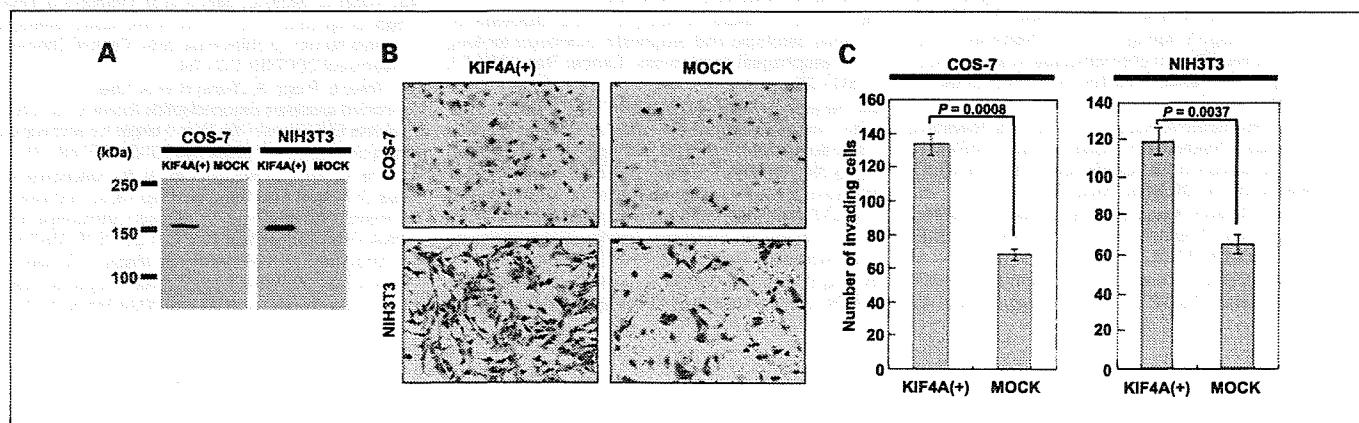Fig. 4. Enhancement of cellular invasiveness by KIF4A introduction into mammalian cells. *A*, transient expression of KIF4A in COS-7 and NIH3T3 cells, detected by Western blot analysis. *B* and *C*, assays demonstrating the invasive nature of NIH3T3 and COS-7 cells in Matrigel matrix after transfection with expression plasmids for human KIF4A. Giemsa staining (*B*; magnification, ×100), and the relative number of cells migrating through the Matrigel-coated filters (*C*). Assays were done thrice and in triplicate wells.

antigens, selective inhibition of KIF4A activity by molecular targeted agents could be a promising therapeutic strategy that is expected to have a powerful biological activity against cancer with a minimal risk of adverse events. Moreover, KIF4A antigens may be used as HLA-restricted epitope peptides for cancer vaccines that can induce specific immune responses by cytotoxic T cells against cancer cells with KIF4A expression.

In summary, activation of KIF4A has a specific functional role for growth and/or malignant phenotype of cancer cells. KIF4A overexpression in resected specimens may be a useful index for application of adjuvant therapy to the patients who are likely to have poor prognosis. In addition, the data strongly imply the possibility of designing new anticancer drugs to specifically target the oncogenic activity of KIF4A for treatment of lung cancer patients.

References

1. Greenlee RT, Hill-Harmon MB, Murray T, Thun M. Cancer statistics, 2001. CA Cancer J Clin 2001;51:15–36.
2. Sozzi G. Molecular biology of lung cancer. Eur J Cancer 2001;37 Suppl 7:S63–73.
3. Morita T, Sugano H. A statistical analysis of lung cancer registered in the Annual of Pathological Autopsy Cases in Japan between 1958 and 1987, with special reference to the characteristics of lung cancer in Japan. Acta Pathol Jpn 1990;40:665–75.
4. Simon GR, Wagner H. Small cell lung cancer. Chest 2003;123 Suppl 1:S259–71.
5. Parkin DM. Global cancer statistics in the year 2000. Lancet Oncol 2001;2:533–43.
6. Chute JP, Chen T, Feigal E, Simon R, Johnson BE. Twenty years of phase III trials for patients with extensive-stage small-cell lung cancer: perceptible progress. J Clin Oncol 1999;17:1794–1801.
7. Sandler AB. Chemotherapy for small cell lung cancer. Semin Oncol 2003;30:9–25.
8. Kikuchi T, Daigo Y, Katagiri T, et al. Expression profiles of non-small cell lung cancers on cDNA microarrays: identification of genes for prediction of lymph-node metastasis and sensitivity to anti-cancer drugs. Oncogene 2003;22:2192–205.
9. Kakiuchi S, Daigo Y, Tsunoda T, Yano S, Sone S, Nakamura Y. Genome-wide analysis of organ-preferential metastasis of human small cell lung cancer in mice. Mol Cancer Res 2003;1:485–99.
10. Kakiuchi S, Daigo Y, Ishikawa N, et al. Prediction of sensitivity of advanced non-small cell lung cancers to gefitinib (Iressa, ZD1839). Hum Mol Genet 2004;13:3029–43.
11. Kikuchi T, Daigo Y, Ishikawa N, et al. Expression profiles of metastatic brain tumor from lung adenocarcinomas on cDNA microarray. Int J Oncol 2006;28:799–805.
12. Taniwaki M, Daigo Y, Ishikawa N, et al. Gene expression profiles of small-cell lung cancers: molecular signatures of lung cancer. Int J Oncol 2006;29:567–75.
13. Yamabuki T, Daigo Y, Kato T, et al. Genome-wide gene expression profile analysis of esophageal squamous-cell carcinomas. Int J Oncol 2006;28:1375–84.
14. Ochi K, Daigo Y, Katagiri T, et al. Prediction of response to neoadjuvant chemotherapy for osteosarcoma by gene-expression profiles. Int J Oncol 2004;24:647–55.
15. Saito-Hisaminato A, Katagiri T, Kakiuchi S, Nakamura T, Tsunoda T, Nakamura Y. Genome-wide profiling of gene expression in 29 normal human tissues with a cDNA microarray. DNA Res 2002;9:35–45.
16. Ochi K, Daigo Y, Katagiri T, et al. Expression profiles of two types of human knee joint cartilage. J Hum Genet 2003;48:177–82.
17. Suzuki C, Daigo Y, Kikuchi T, Katagiri T, Nakamura Y. Identification of COX17 as a therapeutic target for

non-small cell lung cancer. Cancer Res 2003;63:7038–41.
18. Ishikawa N, Daigo Y, Yasui W, et al. ADAM8 as a novel serological and histochemical marker for lung cancer. Clin Cancer Res 2004;10:8363–70.
19. Kato T, Daigo Y, Hayama S, et al. A novel human tRNA-dihydrouridine synthase involved in pulmonary carcinogenesis. Cancer Res 2005;65:5638–46.
20. Furukawa C, Daigo Y, Ishikawa N, et al. Plakophilin 3 oncogene as prognostic marker and therapeutic target for lung cancer. Cancer Res 2005;65:7102–10.
21. Ishikawa N, Daigo Y, Takano A, et al. Increases of amphiregulin and transforming growth factor-α in serum as predictors of poor response to gefitinib among patients with advanced non-small cell lung cancers. Cancer Res 2005;65:9176–84.
22. Suzuki C, Daigo Y, Ishikawa N, et al. ANLN plays a critical role in human lung carcinogenesis through the activation of RHOA and by involvement in the phosphoinositide 3-kinase/AKT pathway. Cancer Res 2005;65:11314–25.
23. Ishikawa N, Daigo Y, Takano A, et al. Characterization of SEZ6L2 cell-surface protein as a novel prognostic marker for lung cancer. Cancer Sci 2006;97:737–45.
24. Takahashi K, Furukawa C, Takano A, et al. The neuromedin u-growth hormone secretagogue receptor 1b/neurotensin receptor 1 oncogenic signaling pathway as a therapeutic target for lung cancer. Cancer Res 2006;66:9408–19.
25. Hayama S, Daigo Y, Kato T, et al. Activation of CDCA1-2, members of centromere protein complex, involved in pulmonary carcinogenesis. Cancer Res 2006;66:10339–48.
26. Kato T, Hayama S, Yamabuki Y, et al. Increased expression of insulin-like growth factor-II messenger RNA-binding protein 1 is associated with tumor progression in patients with lung cancer. Clin Cancer Res 2007;13:434–42.
27. Suzuki C, Takahashi K, Hayama S, et al. Identification of Myc-associated protein with JmjC domain as a novel therapeutic target oncogene for lung cancer. Mol Cancer Ther 2007;6:542–551.
28. Yamabuki T, Takano A, Hayama S, et al. Dickkopf-1 as a novel serologic and prognostic biomarker for lung and esophageal carcinomas. Cancer Res 2007;67:2517–25.
29. Hayama S, Daigo Y, Yamabuki T, et al. Phosphorylation and activation of cell division cycle associated 8 by aurora kinase B plays a significant role in human lung carcinogenesis. Cancer Res 2007;67:4113–22.
30. Kato T, Sato N, Hayama S, et al. Activation of HJURP (Holliday junction-recognizing protein) involved in the chromosomal stability and immortality of cancer cells. Cancer Res 2007;67:8544–53.
31. Zhu C, Jiang W. Cell cycle-dependent translocation of PRC1 on the spindle by Kif4 is essential for midzone

formation and cytokinesis. Proc Nat Acad Sci U S A 2005;102:343–8.
32. Miki H, Okada Y, Hirokawa N. Analysis of the kinesin superfamily: insights into structure and function. Trends Cell Biol 2005;15:467–76.
33. Lee YM, Kim W. Association of human kinesin superfamily protein member 4 with BRCA2-associated factor 35. Biochem J 2003;374:497–503.
34. Narayan G, Bourdon V, Chaganti S, et al. Gene dosage alterations revealed by cDNA microarray analysis in cervical cancer: identification of candidate amplified and overexpressed genes. Genes Chromosomes Cancer 2007;46:373–84.
35. Chin SF, Daigo Y, Huang HE, et al. A simple and reliable pretreatment protocol facilitates fluorescent *in situ* hybridisation on tissue microarrays of paraffin wax embedded tumour samples. Mol Pathol 2003;56:275–9.
36. Callagy G, Cattaneo E, Daigo Y, et al. Molecular classification of breast carcinomas using tissue microarrays. Diagn Mol Pathol 2003;12:27–34.
37. Callagy G, Pharoah P, Chin SF, et al. Identification and validation of prognostic markers in breast cancer with the complementary use of array-CGH and tissue microarrays. J Pathol 2005;205:388–96.
38. Ranson M, Hammond LA, Ferry D, et al. ZD1839, a selective oral epidermal growth factor receptor-tyrosine kinase inhibitor, is well tolerated and active in patients with solid, malignant tumors: results of a phase I trial. J Clin Oncol 2002;20:2240–50.
39. Lawrence CJ, Dawe RK, Christie KR, et al. A standardized kinesin nomenclature. J Cell Biol 2004;167:19–22.
40. Midorikawa R, Takei Y, Hirokawa N. KIF4 motor regulates activity-dependent neuronal survival by suppressing PARP-1 enzymatic activity. Cell 2006;125:371–83.
41. Hirokawa N. Kinesin and dynein superfamily proteins and the mechanism of organelle transport. Science 1998;279:519–26.
42. Miki H, Setou M, Kaneshiro K, Hirokawa N. All kinesin superfamily protein, KIF, genes in mouse and human. Proc Natl Acad Sci U S A 2001;98:7004–11.
43. Muller C, Gross D, Sarli V, et al. Inhibitors of kinesin Eg5: antiproliferative activity of monastrol analogues against human glioblastoma cells. Cancer Chemother Pharmacol 2007;59:157–64.
44. Koller E, Propp S, Zhang H, et al. Use of a chemically modified antisense oligonucleotide library to identify and validate Eg5 (kinesin-like 1) as a target for antineoplastic drug development. Cancer Res 2006;66:2059–66.
45. Zhu C, Zhao J, Bibikova M, et al. Functional analysis of human microtubule-based motor proteins, the kinesins and dyneins, in mitosis/cytokinesis using RNA interference. Mol Biol Cell 2005;16:3187–99.
46. Mazumdar M, Sundareshan S, Misteli T. Human chromokinesin KIF4A functions in chromosome condensation and segregation. J Cell Biol 2004;166:613–20.

—656—

Fibroblast growth factor receptor 1 oncogene partner as a novel prognostic biomarker and therapeutic target for lung cancer

Yuria Mano,[1] Koji Takahashi,[1] Nobuhisa Ishikawa,[1] Atsushi Takano,[1] Wataru Yasui,[2] Kouki Inai,[3] Hitoshi Nishimura,[4] Eiju Tsuchiya,[5] Yusuke Nakamura[1,6] and Yataro Daigo[1]

[1]Laboratory of Molecular Medicine, Human Genome Center, Institute of Medical Science, The University of Tokyo, 4-6-1 Shirokanedai, Minato-ku, Tokyo 108-8639; Departments of [2]Molecular Pathology and [3]Pathology, Graduate School of Biomedical Sciences, Hiroshima University, 1-2-3 Kasumi, Minami-Ku, Hiroshima 734-8551; [4]Department of Thoracic Surgery, Saitama Cancer Center, 818 Ina-machi, Kita-Adachi-gun, Saitama 362-0806; [5]Kanagawa Cancer Center Research Institute, 1-1-2 Nakao, Asahi-ku, Yokohama 241-0815, Japan

To screen candidate molecules that might be useful as diagnostic biomarkers or for development of novel molecular-targeting therapies, we previously carried out gene-expression profile analysis of 101 lung carcinomas and detected an elevated expression of FGFR1OP (fibroblast growth factor receptor 1 oncogene partner) in the majority of lung cancers. Immunohistochemical staining using tumor tissue microarrays consisting of 372 archived non-small cell lung cancer (NSCLC) specimens revealed positive staining of FGFR1OP in 334 (89.8%) of 372 NSCLCs. We also found that the high level of FGFR1OP expression was significantly associated with shorter tumor-specific survival times ($P < 0.0001$ by log-rank test). Moreover, multivariate analysis determined that FGFR1OP was an independent prognostic factor for surgically treated NSCLC patients ($P < 0.0001$). Treatment of lung cancer cells, in which endogenous FGFR1OP was overexpressed, using FGFR1OP siRNA, suppressed its expression and resulted in inhibition of the cell growth. Furthermore, induction of FGFR1OP increased the cellular motility and growth-promoting activity of mammalian cells. To investigate its function, we searched for FGFR1OP-interacting proteins in lung cancer cells and identified ABL1 (Abelson murine leukemia viral oncogene homolog 1) and WRNIP1 (Werner helicase interacting protein 1), which was known to be involved in cell cycle progression. FGFR1OP significantly reduced ABL1-dependent phosphorylation of WRNIP1 and resulted in the promotion of cell cycle progression. Because our data imply that FGFR1OP is likely to play a significant role in lung cancer growth and progression, FGFR1OP should be useful as a prognostic biomarker and probably as a therapeutic target for lung cancer. (*Cancer Sci* 2007; 98: 1902–1913)

L ung cancer is the leading cause of cancer deaths worldwide, and non-small cell lung cancer (NSCLC) accounts for nearly 80% of those cases.[1] Many genetic alterations associated with development and progression of lung cancers have been reported, but the complex molecular mechanisms of pulmonary carcinogenesis remain largely unclear.[2] Systemic chemotherapy is the main treatment for the majority of patients with NSCLC, because most patients are diagnosed at an advanced stage of the disease. Within the last decade several newly developed cytotoxic agents such as paclitaxel, docetaxel, gemcitabine, and vinorelbine have begun to offer multiple choices for treatment of patients with advanced lung cancer; however, each of those regimens confers only a modest survival benefit compared with cisplatin-based therapies.[3,4] Hence, novel therapeutic strategies such as molecular-targeted drugs and antibodies, and cancer vaccines, are eagerly expected.

Systematic analysis of expression levels of thousands of genes using a cDNA microarray technology is an effective approach for identifying molecules involved in oncogenic pathways or those associated with efficacy of anticancer therapy; some of these genes or their gene products may be promising target molecules for the development of novel therapies and/or tumor biomarkers.[5–11] To identify such molecules, we established a new screening system consisting of the sequential steps of: (i) genome-wide expression profile analysis of 101 lung cancers (NSCLCs and SCLCs), coupled with enrichment of tumor cells by laser microdissection,[5–8,11] and its comparison with the data of the expression profile of 31 normal human tissues (27 adult and four fetal organs);[12,13] and (ii) verification of the biomedical and clinicopathological significance of the respective gene products by tumor-tissue microarray analysis of hundreds of archived lung-cancer materials, as well as RNA interference (RNAi) technologies.[14–27] This systematic approach revealed that the gene encoding fibroblast growth factor receptor 1 oncogene partner (FGFR1OP alias FOP) was overexpressed in the great majority of primary NSCLCs.

FGFR1OP was originally identified as a fusion partner for FGFR1 in the t(6;8)(q27;p11) chromosomal translocations in myeloproliferative disorders (MSD).[28–30] However, the biological roles of FGFR1OP during lung carcinogenesis have not been clarified. Werner helicase interacting protein 1 (WRNIP1 alias WHIP) was known to physically interact with WRN (Werner syndrome) protein that encodes a member of the RecQ subfamily and the DEAH (Asp-Glu-Ala-His) subfamily of DNA and RNA helicases.[31] WRNIP1 shows homology to replication factor C family proteins, and is conserved from *Escherichia coli* to humans.[32] Studies in yeast and human cells suggest that this gene may affect the aging process and interact with the DNA replication machinery to modulate the function of DNA polymerase δ (POLD) during DNA replication or replication-associated repair.[31,33–35] However, the roles of WRNIP1 in tumorigenesis are also uninvestigated.

In this study, we describe that overexpression of FGFR1OP could contribute to the malignant nature of lung cancer cells and that FGFR1OP significantly reduces ABL1-dependent phosphorylation of WRNIP1 and appears to promote cancer cell cycle progression. We suggest that targeting the FGFR1OP molecule might hold promise for the development of a new diagnostic and therapeutic strategy in the clinical management of lung cancers.

Materials and Methods

Cell lines and clinical tissue samples. Twenty-two human lung-cancer cell lines used in this study were as follows: 18 NSCLC cell lines, A427, A549, LC176, LC319, PC-9, PC-14, NCI-H520, NCI-H522, NCI-H647, NCI-H1373, NCI-H1666,

NCI-H1703, NCI-H2170, RERF-LC-AI, SK-MES-1, SK-LU-1, LU61, and LX1, and four SCLC cell lines, DMS114, DMS273, SBC-3, and SBC-5. All cells were grown in monolayers in appropriate medium supplemented with 10% fetal calf serum (FCS) and maintained at 37°C in an atmosphere of humidified air with 5% CO_2. Human small airway epithelial cells (SAEC) were grown in optimized medium (SAGM) purchased from Cambrex Bio Science Inc. (Walkersville, MD). Surgically resected primary NSCLC samples had been obtained earlier with written informed consent. A total of 372 formalin-fixed samples of primary NSCLCs including 237 adenocarcinomas (ADCs), 94 squamous cell carcinoma (SCCs), 28 large cell carcinomas (LCCs), 13 adenosquamous carcinomas (ASCs) and adjacent normal lung tissues, had been obtained earlier along with clinicopathological data from patients who had a curative surgical operation at Saitama Cancer Center (Saitama, Japan). Lung cancer specimens and five adult tissues (heart, liver, lung, kidney, and testis) from postmortem materials (two individuals with NSCLC) had been obtained earlier at Hiroshima University (Hiroshima, Japan). The histological classification of the tumor specimens was carried out by the WHO criteria.[36] This study and the use of all clinical materials were approved by the Institutional Research Ethics Committees.

Semiquantitative RT-PCR analysis. Total RNA was extracted from cultured cells and clinical tissues using Trizol reagent (Life Technologies, Inc. Gaithersburg, MD) according to the manufacturer's protocol. Extracted RNAs and normal human-tissue polyA RNAs were treated with DNase I (Roche Diagnostics, Basel, Switzerland) and then reversely transcribed using oligo $(dT)_{12-18}$ primer and SuperScript II reverse transcriptase (Life Technologies). Semiquantitative reverse transcription-polymerase chain reaction (RT-PCR) experiments were carried out with synthesized *FGFR1OP* gene-specific primers (5'-CTGCTGGTACGTGTGATCTTTG-3' and 5'-ACCTTAATG-GTCTAACAAACCTTCC-3'), or with β-actin (*ACTB*)-specific primers (5'-ATCAAGATCATTGCTCCTCCT-3' and 5'-CTG-CGCAAGTTAGGTTTTGT-3'). PCR reactions were optimized for the number of cycles to ensure product intensity within the logarithmic phase of amplification.

Northern-blot analysis. Human multiple-tissue blot (23 normal tissues including heart, brain, placenta, lung, liver, skeletal muscle, kidney, pancreas, spleen, thymus, prostate, testis, ovary, small intestine, colon, peripheral blood leukocyte, stomach, thyroid, spinal cord, lymph node, trachea, adrenal gland, and bone marrow; BD Biosciences Clontech, Palo Alto, CA) was hybridized with a ^{32}P-labeled PCR product of *FGFR1OP*. The cDNA probes of *FGFR1OP* were prepared by RT-PCR using primers, 5'-TAAT-AGTACCAGCCATCGCTCAG-3' and 5'-ATCCTACGGCTTT-ATTGACACCT-3'. Pre-hybridization, hybridization, and washing were carried out according to the supplier's recommendations. The blots were autoradiographed with intensifying screens at –80°C for one week.

Preparation of anti-FGFR1OP polyclonal antibody. Rabbit antibodies specific to FGFR1OP were raised by immunizing rabbits with histidine-tagged human FGFR1OP protein (codons 7–173; accession No. NM_007045), and purified with standard protocols using affinity columns (Affi-gel 10; Bio-Rad Laboratories, Hercules, CA) conjugated with the histidine-tagged protein. On Western blots we confirmed that the antibody was specific to FGFR1OP, using lysates from NSCLC tissues and cell lines as well as normal lung tissues.

Western-blot analysis. Cells were lyzed with radioimmuno-precipitation (RIPA) buffer (50 mM Tris-HCl [pH 8.0], 150 mM NaCl, 1% NP-40, 0.5% deoxychorate-Na, 0.1% sodium dodecyl sulphate [SDS]) containing protease inhibitor (Protease Inhibitor Cocktail Set III; CALBIOCHEM). Protein samples or immunoprecipitates were separated by SDS-polyacrylamide gels and electroblotted onto Hybond-ECL nitrocellulose membranes (GE Healthcare Bio-sciences). Blots were incubated with a rabbit polyclonal anti-FGFR1OP antibody, a mouse monoclonal FGFR1OP antibody (Abnova Corporation), a rabbit polyclonal WRNIP1 antibody (Abcam), a rabbit polyclonal ABL1 antibody (Cell Signaling Technology), a mouse monoclonal β-actin (ACTB) antibody (Sigma), or a mouse monoclonal anti-c-Myc antibody (Santa Cruz). Antigen-antibody complexes were detected using secondary antibodies conjugated to horseradish peroxidase (GE Healthcare Bio-sciences). Protein bands were visualized by enhanced chemiluminescence (ECL) western blotting detection reagents (GE Healthcare Bio-sciences), as previously described.[20]

Immunofluorescence analysis. Cultured cells were fixed with ice-cold methanol : acetone for 10 min at –20°C and subsequently washed with phosphate-buffered saline (PBS) (–). Prior to the primary antibody reaction, fixed cells were covered with CAS-BLOCK (ZYMED Laboratories) for 10 min to block non-specific antibody binding. Then the cells were incubated with a mouse monoclonal FGFR1OP antibody (Abnova Corporation), a rabbit polyclonal anti-WRNIP1 (Abcam) and a rabbit polyclonal ABL1 antibody (Santa Cruz Biotechnology). Antibodies were stained with an antimouse secondary antibody conjugated to Alexa Fluor 488 (Molecular Probes) and an antirabbit secondary antibody conjugated to Alexa Fluor 594 (Molecular Probes). DNA was stained with 4'6'-diamidino-2-phenylindole dihydrochloride (DAPI). To determine the cell cycle-dependent localization of FGFR1OP, synchronization at the G1–S boundary was achieved with aphidicolin block. Cells were blocked with 1 μg/mL of aphidicolin (Sigma-Aldrich) for 24 h, and released from the block by four washes with PBS. These cells were cultured in medium and harvested for analysis at 1.5, 4.0 and 9.0 h after release from the cell-cycle arrest. Images were viewed and assessed using a confocal microscope at wavelengths of 488, 594 nm (TCS SP2 AOBS: Leica Microsystems).

Flow cytometry. Cells were trypsinized, collected in PBS and fixed in 70% cold ethanol for 30 min. After treatment with 100 μg/mL of RNase (Sigma-Aldrich), the cells were stained with 50 μg/mL of propidium iodide (Sigma-Aldrich) in PBS. Flow cytometry was carried out on a Becton Dickinson FACScan and analyzed with ModFit software (Verity Software House, Topsham, ME). The cells selected from at least 20 000 ungated cells were analyzed for DNA content.

Immunohistochemistry and tissue microarray. Tumor-tissue microarrays were constructed using 372 formalin-fixed primary NSCLCs, as published previously.[37–39] The tissue area for sampling was selected by visual alignment with the corresponding HE-stained section on a slide. Three, four, or five tissue cores (diameter 0.6 mm; height 3–4 mm) taken from a donor tumor block were placed into a recipient paraffin block using a tissue microarrayer (Beecher Instruments, Sun Prairie, WI). A core of normal tissue was punched from each case, and 5-μm sections of the resulting microarray block were used for immunohistochemical analysis.

To investigate the presence of FGFR1OP protein in clinical samples that had been embedded in paraffin blocks, we stained the sections as previously described.[18,20,25] Briefly, a rabbit polyclonal antihuman FGFR1OP antibody was added after blocking of endogenous peroxidase and proteins. The sections were incubated with HRP-labeled antirabbit IgG as the secondary antibody. Substrate-chromogen was added and the specimens were counterstained with hematoxylin.

Three independent investigators assessed FGFR1OP positivity semiquantitatively without prior knowledge of clinicopathological data. The intensity of FGFR1OP staining was evaluated using the following criteria: strong positive (2+), dark brown staining in more than 50% of tumor cells completely obscuring nucleus and cytoplasm; weak positive (1+), any lesser degree of brown staining appreciable in nucleus and cytoplasm; absent (scored as 0), no appreciable staining in tumor cells. Cases were accepted